Long-term observational characteristics of different severe convective wind types around Australia

Andrew Brown,[a,c] Andrew Dowdy,[b,c] Todd P. Lane,[a,c] Stacey Hitchcock,[a,c]

[a] *ARC Centre of Excellence for Climate Extremes, The University of Melbourne, Australia*

[b] *Australian Bureau of Meteorology, Melbourne, Australia*

[c] *School of Geography, Earth and Atmospheric Sciences, The University of Melbourne, Australia*

Corresponding author: Andrew Brown, andrewb1@student.unimelb.edu.au

ABSTRACT: Regional understanding of severe surface winds produced by convective processes (severe convective winds: SCWs) is important for decision making in several areas of society, including weather forecasting and engineering design. Meteorological studies have demonstrated that SCWs can occur due to a number of different mesoscale and microscale processes, in a range of large-scale atmospheric environments. However, long-term observational studies of SCW characteristics often have not considered this diversity in physical processes, particularly in Australia. Here, a statistical clustering method is used to separate a large dataset of SCW events, measured by automatic weather stations around Australia, into three types, associated with strong background wind, steep lapse rate, and high moisture environments. These different types of SCWs are shown to have different seasonal and spatial variations in their occurrence, as well as different measured wind gust, lightning, and parent-storm characteristics. In addition, various convective diagnostics are tested in their ability to discriminate between measured SCW events and non-severe events, with significant variations in skill between event types. Differences in environmental conditions and wind gust characteristics between clusters suggests potentially different physical processes for SCW production. These findings are intended to improve regional understanding of severe wind characteristics, as well as environmental prediction of SCWs in weather and climate applications, by considering different event types.

SIGNIFICANCE STATEMENT: The purpose of this study is to improve regional understanding of different types of severe wind events in Australia, specifically those associated with atmospheric convection. We did this by constructing a dataset of 413 severe convective wind events, using weather station and radar data within 20 regions around Australia. We then split those events into three different types, based on the environmental conditions that they occur within. We found that each event type tends to occur at different times of the year and in different regions, while also having different wind gust and lightning characteristics. In addition, the atmospheric conditions that are helpful for prediction of severe wind events differs between each type. These results are intended to be useful for prediction of severe wind events associated with convection and assessing their variability, characteristics, and impacts, in both weather forecasting and climate analysis.

This Work has been accepted to Weather and Forecasting (https://doi.org/10.1175/WAF-D-23-0069.1). The AMS does not guarantee that the copy provided here is an accurate copy of the Version of Record (VoR).

1. Introduction

Severe surface winds associated with non-tornadic convective processes (severe convective winds: SCWs) are a hazard that can have impacts on several aspects of society, including aviation operations (Potts et al. 2010; Fujita 1983), fire management (Tory and Thurston 2015), energy networks (Savory et al. 2001), and residential buildings (Jesson et al. 2015). For example, in Australia, SCWs associated with thunderstorms have contributed to electricity transmission network failures affecting entire states (Australian Energy Market Operator 2020). Improved understanding of the physical processes that lead to SCWs is important for helping enhance preparedness for these events. In addition, assessments of the spatial and temporal variability of these events, and their intensity, can help with design purposes and future planning.

SCWs can occur due to a wide range of mesoscale and microscale mechanisms, in different large-scale environments, as demonstrated by several studies including in Australia. Mesoscale processes include downbursts that are produced by intense, convective downdrafts (Wakimoto 1985; Atkins and Wakimoto 1991), internal mesoscale convective system (MCS) circulations (Weisman 1992), MCS outflow (Johns and Hirt 1987), supercell downdrafts (Klemp and Rotunno 1983), and downdrafts within extratropical cyclones and synoptic-scale fronts (Clark 2013; Earl et al. 2017). These mesoscale processes are related to several microscale processes, including evaporative cooling from precipitation, precipitation loading, and the associated potential for horizontal momentum transport (Mahoney et al. 2009; Geerts 2001), with variations in the relative contribution of these processes between events, as suggested by modelling and observational studies (Proctor 1989; Sherburn et al. 2021). SCWs can occur under a range of large-scale environmental conditions, such as with high amounts of convective available potential energy (CAPE) and low amounts of vertical wind shear (Miller and Mote 2018) and with low amounts of CAPE and high amounts of vertical wind shear (Sherburn and Parker 2014). Although many of the studies mentioned above have focused on the United States and Europe, studies in eastern and tropical Australia have demonstrated similar mesoscale and microscale processes leading to severe surface winds for individual cases, including supercells (Richter et al. 2014), bow echoes (Earl and Simmonds 2018), and downbursts (Sherman 1987; Keenan and Carbone 1992; Potts et al. 2010; Brown et al. 2023).

Long-term observational studies of thunderstorms and SCWs often use classification methods to separate these different processes. These studies are often based around classification of convective storm types using radar information (Gallus et al. 2008; Smith et al. 2013; Gatzen 2013; Yang and Sun 2018) and/or clustering of the large-scale environment or synoptic weather types (Pacey et al. 2021; Zhou et al. 2021; Morgenstern et al. 2023). Classification methods such as these can reveal different spatial and temporal variations in the occurrence of different storm types and environments, while also providing insights on methods for the detection or prediction of different events. For example, Smith et al. (2013) found that there are different spatial patterns in SCW frequency for events associated with different parent-storm types across the United States, such as quasi-linear convective systems and supercells. Similarly, Cintineo et al. (2020) developed different environmental predictors of SCW events in the United States, that depend on whether the parent storm was classified as linear or cellular based on the amount of environmental wind shear. In contrast to classifications based on convective storm morphology, Sherburn et al. (2021) demonstrated potential seasonal and regional variability in SCW-producing processes over the United States by assessing the ratio between the storm outflow speed and surface wind gust intensity, while Pacey et al. (2021) found that SCWs in Europe during the warm-season tend to have more CAPE and less vertical wind shear than during the cool-season.

However, in Australia very few studies have classified convective processes and environments over long periods, with previous work focusing on specific regions, processes, or hazards. For example, Keenan and Carbone (1992) and Peter et al. (2015) demonstrated that distinct synoptic weather types in Darwin (tropical Australia) and Sydney (sub-tropical east coast), respectively, can lead to different observed convective storm characteristics observed by radar. Similarly, Soderholm et al. (2017) examined hailstorms in southeast Queensland (coastal sub-tropical Australia), and found different hailstorm occurrence frequencies and characteristics within different synoptic weather regimes, while also highlighting the role of sea breezes for storm initiation in this region. Keenan and Carbone (1992) and Short et al. (2022) also showed that the phase of the northern Australia monsoon can influence the morphology of convective systems near Darwin, as diagnosed from radar. Hitchcock et al. (2021) classified the storm-scale structures associated with heavy rainfall events near Melbourne (south-east Australia). They identified linear systems using radar, finding that they coincide with most extreme rainfall days in that region. However, no previous study

has classified the different types of convective storms and environments for SCWs using long-term data, despite SCWs receiving a significant amount of attention in southeastern Australia (Geerts 2001; Spassiani and Mason 2021; Holmes 2002; El Rafei et al. 2023). This has resulted in significant regional knowledge gaps in understanding the most relevant physical processes for SCWs in Australia, as well as in the development of regional environmental methods for SCW prediction for weather and climate applications (Allen and Allen 2016; Brown and Dowdy 2021b), noting that environmental factors for convective hazards can vary significantly across different regions (Taszarek et al. 2020a; Dowdy and Brown 2023).

In addition to these uncertainties related to different convective storm types and processes for SCWs in Australia, there is also a lack of knowledge related to the diversity in wind gust characteristics and lightning occurrences associated with different types of SCWs, globally. For example, differences in wind gust statistics between convective processes, such as the extreme wind speed distribution and temporal gust characteristics that are relevant in engineering design, have not been quantified using long-term statistics (Lombardo and Zickar 2020). Similarly, the amount of lightning could also potentially vary with the different mesoscale and microscale SCW processes outlined above, with lightning occurrence sometimes used as a method for detection of SCWs in weather forecasting (Thompson et al. 2021) and climatological studies (Mohr et al. 2017; Brown and Dowdy 2021a). Although the amount of lightning associated with individual SCW cases has been examined, including cases associated with both high and low/zero amounts of lightning (Goodman et al. 1988; van den Broeke et al. 2005; Brown et al. 2023), this has yet to be quantified anywhere in the world using long-term observations.

This study will build on previous literature by considering the characteristics of different SCW event types in Australia using long-term data, including the classification of parent storms and the large-scale environment, as well as examining surface wind gust and lightning characteristics. Here, SCWs are defined by station wind gust measurements, with associated radar reflectivity data used to identify convective processes. Following Brown et al. (2023), three SCW event types will be defined based on large-scale environmental conditions, using a statistical clustering technique. This includes SCW events associated with: strong background wind, steep lapse rate, and high moisture environments. In addition, parent-storm types are classified based on reflectivity structures and

Doppler velocity data, to provide further insights into the relevant mesoscale processes for different SCW types. The research questions that this study examines are as follows:

- How frequently do different types of SCWs occur in Australia and does this vary spatially and seasonally?
- How do the SCW types differ in their wind gust characteristics and parent storm types?
- What is the probability of lightning occurrence associated with each type of SCW event?
- What are the relevant diagnostics for discriminating between SCWs and non-severe events, and do these vary between types of SCW events and types of parent storms?

This paper is structured as follows: Firstly, a description of data and methods is presented, including our SCW definition based on measured wind gusts and radar reflectivity data, details on event clustering and parent storm classification, and other methods for assessing the long-term characteristics of each type of SCW event. Results are then presented including a SCW climatology that documents the variability, wind gust characteristics, and environmental conditions for each event type. This is followed by discussion of results and conclusions.

2. Data and Methods

a. Severe convective wind event database

Severe convective wind (SCW) events are defined here by a gust (3-second average wind speed at a height of 10 m) of at least 25 m/s, measured by an Automatic Weather Station (AWS) within the observational network managed by the Australian Bureau of Meteorology (the ”Bureau”). Bureau AWS report 3-second gusts as maxima over one-minute intervals. The following two conditions are used to associate severe wind gusts with convective processes:

1. A radar-derived parent storm is within 10 km of the gust, within the previous 10 minutes (see below for definition of parent storm).
2. The ratio of the 3-second gust, reported as one minute maxima, to the 4-hour centered mean is two or greater. This ratio is referred to as the peak-to-mean wind gust ratio.

The gust threshold of 25 m/s is chosen to align with weather forecasting practices in this region, and is similar to severe wind thresholds in previous studies (Spassiani and Mason 2021;

Mohr et al. 2017; Sherburn et al. 2021). The application of the first condition for identifying convective processes is consistent with several studies that use radar reflectivity to assess the origin of convective wind gusts (Smith et al. 2013; Spassiani and Mason 2021). A 10 km storm proximity is chosen based on the knowledge that gust fronts can propagate away from the storm (Lagerquist et al. 2017), while the choice of a 10-minute temporal proximity represents the typical maximum interval between complete scans for radars in the Australian operational network archive. The second condition (peak-to-mean wind gust ratio of at least 2) is used to remove strong gusts that have a nearby storm but are not associated with convection, based on convective gusts being strong and transient compared with the background flow, relative to gusts driven by synoptic-scale pressure gradients (De Gaetano et al. 2014). Although the appropriate threshold for this criteria might be sensitive to the type of event and the local-scale topography associated with individual AWS sites, the value of 2 used here provides some consistency with previous studies (Durañona et al. 2007; El Rafei et al. 2023), and appears to be a reasonable criteria for defining SCWs based on inspecting individual events in this dataset (not shown).

For identifying parent storms, a set of 20 radars is used, with these radars located around Australia as shown in Figure 1. These locations have been grouped into tropical, east coast, south coast, and inland locations, also indicated in Figure 1. These radars were chosen based on having at least 6 years of archived reflectivity and Doppler velocity data within the Australia Unified Radar Archive (AURA, Soderholm et al. (2022)), and are listed in Table 1. Data for each radar from AURA are available on a unique three-dimensional grid, with 1 km spacing in the horizontal and 500 m spacing in the vertical. Further details on this dataset can be found from Soderholm et al. (2022). Parent storms are identified through the segmentation of column maximum radar reflectivity. First, a Gaussian smoothing filter is applied, and then all potential parent storms are identified by applying a reflectivity threshold of 30 dBZ. Storms are then filtered by applying depth, area, and volume thresholds of 2 km, 15 km^2, and 30 km^3, respectively, to remove ground clutter. Parent storms are associated with a gust if any part of the storm is within 10 km and 10 minutes, as discussed above. Finally, storms are tracked in time based on the original (non-smoothed) reflectivity data, and storm statistics are calculated for further analysis (detailed in Section 2c).

For gust measurements, one-minute maximum wind data are used up until to the end of the year 2020, for all Bureau AWS sites that are within 100 km of the radars listed in Table 1. All Bureau

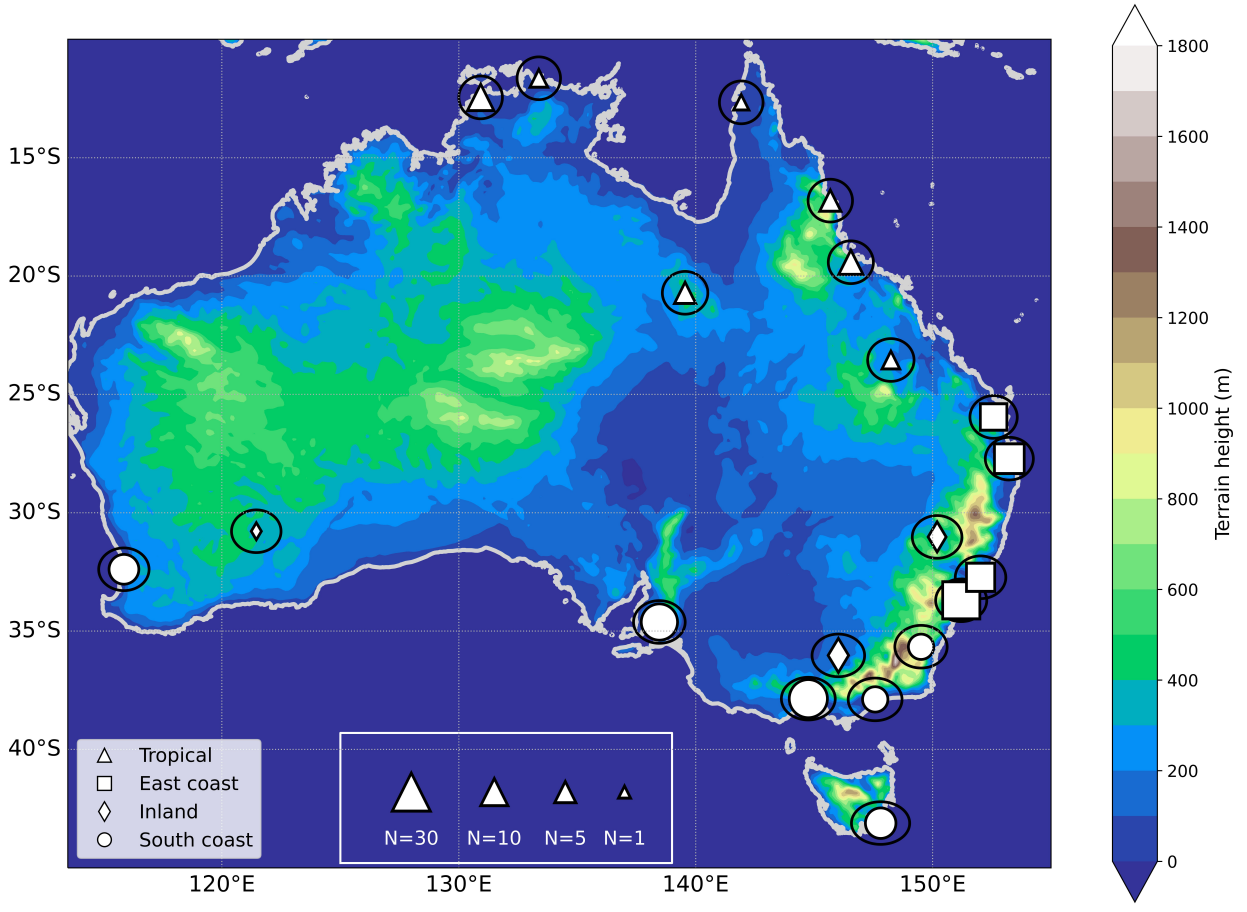

181 FIG. 1. Map of radar locations used in this study. The size of the markers represents the number of
182 automatic weather stations within 100 km of each radar. A 100 km range ring is also shown around each radar
183 location. Different markers are used for locations grouped here as tropical (triangles), east coast (squares), inland
184 (diamonds) and south coast (circles). Terrain heights are provided by the Bureau of Meteorology Atmospheric
185 Regional Reanalysis for Australia, with a 12 km grid spacing (Su et al. 2020).

192 wind gust data are accompanied by quality information, with data only retained for this study if
193 quality checks are flagged as performed, and the data passes the check (98% of the total wind gust
194 data). In addition to this automatic quality control process based on information provided with the
195 data, some erroneously strong gusts were manually removed, upon inspection of the wind gust time
196 series. There was only one tornado measured in this wind gust dataset, in the Sydney radar domain
197 on 16 December 2015 (Richter et al. 2016). This event is excluded here given that non-tornadic
198 wind gusts are the target of this study. Stations are excluded from this study if they are located
199 more than 1000 m above sea level, or if they are located offshore. Stations at high elevation are

Radar ID	Radar name	Radar archive start year	Radar latitude	Radar longitude	Location group	Number of AWS within 100 km	AWS-years	Number of SCW events	Events per AWS-year
2	Melbourne	2008	-37.8553	144.7555	South coast	30	311.1	85	0.27
4	Newcastle	2013	-32.7298	152.0254	East coast	11	71.6	18	0.25
8	Gympie	2007	-25.9574	152.5768	East coast	9	85.8	20	0.23
19	Cairns	2014	-16.8170	145.6830	Tropical	5	31.2	0	0.00
40	Canberra (Captains Flat)	2013	-35.6614	149.5122	South coast	8	63.1	10	0.16
48	Kalgoorlie	2014	-30.7843	121.4548	Inland	1	6.7	4	0.60
49	Yarrawonga	2006	-36.0296	146.0228	Inland	7	77.4	21	0.27
63	Darwin (Berrimah)	2001	-12.4570	130.9250	Tropical	9	81.0	26	0.32
64	Adelaide (Buckland Park)	2005	-34.6169	138.4689	South coast	24	254.1	26	0.10
66	Brisbane (Mt Stapylton)	2006	-27.7178	153.2400	East coast	13	131.2	24	0.18
68	Bairnsdale	2014	-37.8876	147.5755	South coast	8	47.3	8	0.17
69	Namoi (Blackjack Mountain)	2010	-31.0236	150.1917	Inland	5	47.3	48	1.02
70	Perth (Serpentine)	2013	-32.3917	115.8670	South coast	13	90.2	16	0.18
71	Sydney (Terrey Hills)	2009	-33.7008	151.2094	East coast	27	257.7	32	0.12
72	Emerald	2010	-23.5498	148.2392	Tropical	3	26.5	12	0.45
73	Townsville (Hervey Range)	2015	-19.4198	146.5509	Tropical	7	33.1	3	0.09
75	Mount Isa	2012	-20.7112	139.5552	Tropical	5	37.0	14	0.38
76	Hobart (Mt Koonya)	2012	-43.1122	147.8057	South coast	14	114.8	45	0.39
77	Warruwi	2012	-11.6485	133.3800	Tropical	3	23.1	0	0.00
78	Weipa	2015	-12.6664	141.9247	Tropical	2	9.7	1	0.10

TABLE 1. List of radars used in this study for identifying parent storms, with locations shown in Figure 1. AWS-years here represents the amount of gust data (in years) that is available for all AWS within 100 km of each radar, that overlaps with radar data availability during the archive period. The radar archive start year corresponds to the first year for which reflectivity and Doppler velocity data are both available.

removed due to topographic influences on wind speeds at those locations (El Rafei et al. 2023), as these processes are outside the scope of this study. Offshore stations are removed due to frequent reporting of strong, persistent wind gusts, that makes the identification of SCWs challenging based

on the definition used here. This results in a total of 204 AWS across all 20 radar domains, with the number of stations in each domain detailed in Table 1, as well as the number of one-minute AWS observations that coincide with available radar data, accumulated across all available stations, in years (AWS-years).

For analysis in this study, the one-minute AWS gust data is placed onto an hourly, 0.25-degree latitude-longitude grid for comparison with environmental data from the ERA5 reanalysis (Section 2b and e), and lightning observations (Section 2d). For each 0.25-degree grid point, the strongest gust during each hour at all neighbouring AWS is retained (where data is available), with a preference given firstly to SCW events, and then for "convective gusts", with a convective gust defined as having an associated parent storm. SCWs in the same radar domain must also be at least one hour apart to be considered a separate event, following Sherburn et al. (2021). The result is 413 events, with the number of events in each radar domain detailed in Table 1, as well as the number of events per AWS-year. For comparison with SCW events, all non-SCW gusts in the resampled hourly dataset will be referred to here as "non-severe" events, while non-severe gusts with an associated parent storm will be referred to as "convective non-severe" events. Note that because convective non-severe events are defined by all convective gusts that aren't SCWs, this dataset will include gusts that exceed 25 m/s and have a wind gust ratio less than two, with these events likely driven by synoptic-scale processes.

b. Environmental clustering

SCWs will be analysed separately in this study for different event types, defined using statistical clustering of large-scale environmental data. Clustering is performed on environmental diagnostics calculated from hourly pressure-level and surface-level data using the ERA5 reanalysis (Hersbach et al. 2020) on a 0.25-degree latitude-longitude grid. The clustering uses a k-means method that is based on a set of 36 SCW events in eastern Australia (Brown et al. 2023). The clustering is performed using the following diagnostics: mean water vapour mixing ratio from 0–1 km above ground level (Qmean01, g/kg), temperature lapse rate from 1–3 km (LR13, K/km), mean wind speed from 0–6 km (Umean06, m/s), and bulk vertical wind shear from 0–6 km (S06, m/s). Clustering is applied to all SCW events and non-severe events based on hourly data, by using ERA5 data from the preceding hour. Also, following Brown et al. (2023), a spatial maximum is

performed for each component of the clustering, in a 50 km radius around each AWS (considering ERA5 land points only).

The sensitivity of this clustering is tested here by training the method based on the 413 events from the dataset described in Section 2a, rather than the 36 cases in Brown et al. (2023). Results are shown in the Supplementary Material (Section S.1), and indicate that this sensitivity is minimal based on similar clustering between the two methods. We choose to retain the clustering method based on those 36 cases (rather than based on the broader set of 413 cases) to provide consistency with Brown et al. (2023), and the physical interpretations of clusters in that study.

Brown et al. (2023) used this clustering to separate SCW events into three subsets in eastern Australia, characterised by:

1. Strong background winds (high Umean06) and relatively dry low-levels (low Qmean01)

2. Steep low-level lapse rates (high LR13), moderate amounts of low-level moisture (moderate Qmean01), and moderately strong background winds (high Umean06)

3. Large amounts of low-level moisture (high Qmean01)

This clustering can be visualised for the events here in the Results section (Figure 2, Section 3a). These clusters represent different ”event types”, and will be referred to here as ”strong background wind”, ”steep lapse rate”, and ”high moisture” events, respectively. As well as having different environmental conditions, events in these clusters tend to be associated with different types of synoptic features and parent storms. The strong background wind cluster was found to often be associated with strong midlatitude cyclones and relatively shallow convection with low CAPE by Brown et al. (2023), based on a set of 6 events. That study also found that the steep lapse rate cluster (based on 11 events) has similar environmental characteristics to microburst events as presented by Wakimoto (1985) for example. The high moisture cluster was found to be associated with deep convective storms, often with high values of radar-derived rotational shear suggesting potential storm rotation and supercells (based on 19 events). These cluster characteristics are summarised in Table 2, including a description of potential physical mechanisms for severe surface wind production in each cluster.

	Strong background wind events	Steep lapse rate events	High moisture events
Environment	Strong 0–6 km winds, relatively dry 0–1 km layer, limited CAPE	Steep 1–3 km lapse rates, moderate low-level moisture, moderate to strong 0–6 km winds, low to moderate CAPE	High 0–1 km moisture content, high CAPE
Synoptic features	Often associated with mid-latitude cyclones	-	-
Parent storm characteristics	Shallow	Moderately deep	Deep and often supercellular
Potential physical mechanisms for SCWs	Shallow convective transport of strong synoptic-scale winds to the surface	Downbursts driven by sub-cloud evaporation/melting	Outflow from deep convective storms including supercell downdrafts

TABLE 2. Summary of severe convective wind event types, based on results from Brown et al. (2023)

c. Radar-derived parent storm statistics

From radar reflectivity and Doppler velocity data, several statistics are derived for parent storms associated with SCW events and convective non-severe events. Most of these storm statistics are defined as instantaneous values at the most recent radar scan before each wind gust. These include morphological statistics based on ellipses fit to column-maximum reflectivity data, giving the major and minor axis lengths, and the corresponding aspect ratio. We also consider the maximum altitude of the parent storm, and the number of local reflectivity maxima within the storm.

In addition, Doppler velocity data are used to derive the ”azimuthal shear”, which can be used to estimate storm rotation. Previous studies have found azimuthal shear to be useful for identifying intense storms leading to SCWs, including rotating supercell storms, noting that other non-meteorological factors can affect this quantity (Cintineo et al. 2020). Azimuthal shear is available in AURA on a 1 km horizontal and 500 m vertical grid, with this study using the 99.5th percentile of azimuthal shear within the parent storm, limited to 2–6 km above ground level. A temporal filter is applied to the 99.5th percentile value, with a rolling 1-hour median used to filter short lived, non-supercellular rotation that may exist along gust fronts, for example. This temporal filter is only applied for parent storms that persist for longer than one radar scan before splitting, merging, or dissipating.

These storm statistics are summarised together using the objective parent-storm classification developed by Brown et al. (2023) for SCWs in eastern Australia based on a set of 36 cases. The classification is as follows, and includes six storm types:

1. Linear: major axis longer than 100 km, and aspect ratio greater than 3.

2. Non-linear: major axis longer than 100 km, and aspect ratio less than 3.

3. Cellular: major axis less than 100 km, and one local reflectivity maximum.

4. Cell cluster: major axis less than 100 km, and more than one local reflectivity maximum.

5. Supercell: major axis length is less than 100 km, 99.5th percentile of azimuthal shear is greater than 0.0040 s^{-1}, and maximum storm height is at least 7 km.

6. Embedded supercell: major axis length is greater than 100 km, 99.5th percentile of azimuthal shear is greater than 0.0040 s^{-1}, and maximum storm height is at least 7 km.

A threshold on maximum height has been added here for supercellular storms, as an addition to the Brown et al. (2023) classification scheme. This was to limit the number of convective non-severe events that are misclassified as supercells, based on the azimuthal shear threshold outlined above. Due to incomplete azimuthal shear data, 5.3% of parent storms associated with SCW events are not able to be classified as supercells or embedded supercells, as well as 10.7% of convective non-severe events, and this is noted as a limitation of this objective method. These events and non-severe events with missing azimuthal shear data are removed from analysis that is based on parent-storm type (parts of Section 3c and Section 3d). For further details on the development of this classification approach, as well as other potential limitations, the reader is referred to Brown et al. (2023). In addition to the instantaneous statistics mentioned above, the speed of the storm is derived using the entire storm track. Storm speed is calculated by using a spatial Thiel-Sen fit, based on the reflectivity-weighted center of the parent storm.

d. Wind gust and lightning statistics

As mentioned in Section 2a, the peak-to-mean gust ratio is analysed for all AWS wind gust observations, and forms one aspect of the SCW event definition. In addition, the ratio of the peak wind gust to mid-level mass-weighted mean wind speed (over the 800–600 hPa layer) is calculated, to estimate the contribution of horizontal momentum aloft to the surface gust intensity. The ratio used here will be referred to as the gust-to-mid-level-wind-speed ratio. It is hypothesised that this ratio should be lower for events driven by vertical mixing of horizontal momentum from aloft to the surface, and higher for SCW events driven by thermodynamic downdraft processes. The

distribution of this ratio for SCW events and non-severe events will be evaluated between event types.

The total number of lightning strokes associated with SCWs, non-severe events, and convective non-severe events is also analysed, using data from the World Wide Lightning Location Network (WWLLN, Virts et al. (2013)). Lightning data are on a hourly, 0.25-degree latitude-longitude grid, representing the total number of strokes observed in each hour (centered on the hour). The nearest temporal lightning observation from the hourly data is associated with each wind gust. The statistics here represent a spatial sum, over all lighting grid points within 50 km of the gust. This spatial proximity definition is consistent with previous studies that have used lightning to investigate convective wind gusts (Mohr et al. 2017).

e. Environmental diagnostics

Environmental diagnostics that are commonly used for identifying favourable conditions for SCWs are investigated here, in terms of their skill in discriminating between SCW events, convective non-severe events, and non-severe events as measured by AWS and defined in Section 2a. This skill is assessed for each of the event types discussed in Section 2b, and for each parent-storm type presented in Section 2c. Firstly, some key environmental wind and thermodynamic diagnostics will be tested by inspecting their distributions for SCWs compared with convective non-severe events. These diagnostics include S06 and Umean06 (as described in Section 2b), as well as downdraft CAPE (DCAPE, Gilmore and Wicker (1998)), and most-unstable CAPE (MUCAPE). DCAPE is often used to estimate the potential for intense downdrafts due to evaporative cooling, while MUCAPE is an estimate of the maximum potential for deep convective updrafts in a column of air. Additional details on the calculation of each diagnostic can be found in the Supplementary Material (Section S.2). As in Section 2b, these variables are calculated from hourly ERA5 data, and represent a 50 km spatial maximum around the gust location. Observed wind gusts are associated with environmental diagnostics using ERA5 data from the preceding hour, unless noted otherwise.

Secondly, a broader set of 48 environmental diagnostics are tested in their ability to discriminate between SCW events and non-severe events, and between SCW events and convective non-severe events, by calculating the relative operating characteristic (ROC) curve and the area under the curve (AUC) score. The set of 48 diagnostics used here are a subset of those considered by Brown

and Dowdy (2021a) for identifying favourable SCW environments, with details of diagnostic formulations presented in the Supplementary Material (Section S.2). Diagnostics include measures of downburst and severe storm potential, as well as instability and wind variables. The ROC and AUC approach is consistent with recent studies that investigate favourable SCW environments (Bolgiani et al. 2020; Romanic et al. 2022), and is considered suitable for assessing discrimination of binary events in the atmospheric sciences (Hogan and Mason 2011). However, it is noted that the ROC and AUC score are not measures of predictive skill as they don't penalise identification bias. Instead, these methods can be viewed as being indicative of the potential predictive skill (Wilks 2001). This should be kept in mind when interpreting these results, as predictions of hazardous convection using environmental diagnostics produce numerous false alarms, as a result of biases in the diagnostic approach and in observations of the hazards being predicted (see Rasmussen and Blanchard (1998) for example).

ROC curves are produced for each diagnostic by plotting the hit rate against the false alarm rate, for a range of diagnostic thresholds. An example curve is shown in the Supplementary Material for a single diagnositc (Section S.3), with some further discussion of the AUC score therein. For testing some diagnostics that are intended to have lower values for SCW events relative to non-severe events (as determined by mean values for SCW events and non-severe events), class labels (SCW event or non-severe event) are reversed prior to producing ROC curves. The AUC score ranges from 0 to 1, with scores above 0.5 representing skillful discrimination, and 1 representing perfect discrimination. Uncertainties are estimated by randomly resampling the SCW event and non-severe event datasets 1,000 times with replacement, and computing the AUC on each sample. This gives a distribution of AUC scores for each diagnostic, representing random variations due to sampling. These distributions are presented visually in the results alongside median AUC scores over these distributions. For computational efficiency, the resampling procedure for non-severe events is done by randomly selecting 10% of the original dataset, for each sample.

3. Results

a. Event climatology

Based on the definition outlined in Section 2a, 413 SCW events are identified by AWS across Australia, with the number of events in each radar location shown in Table 1. These 413 events are

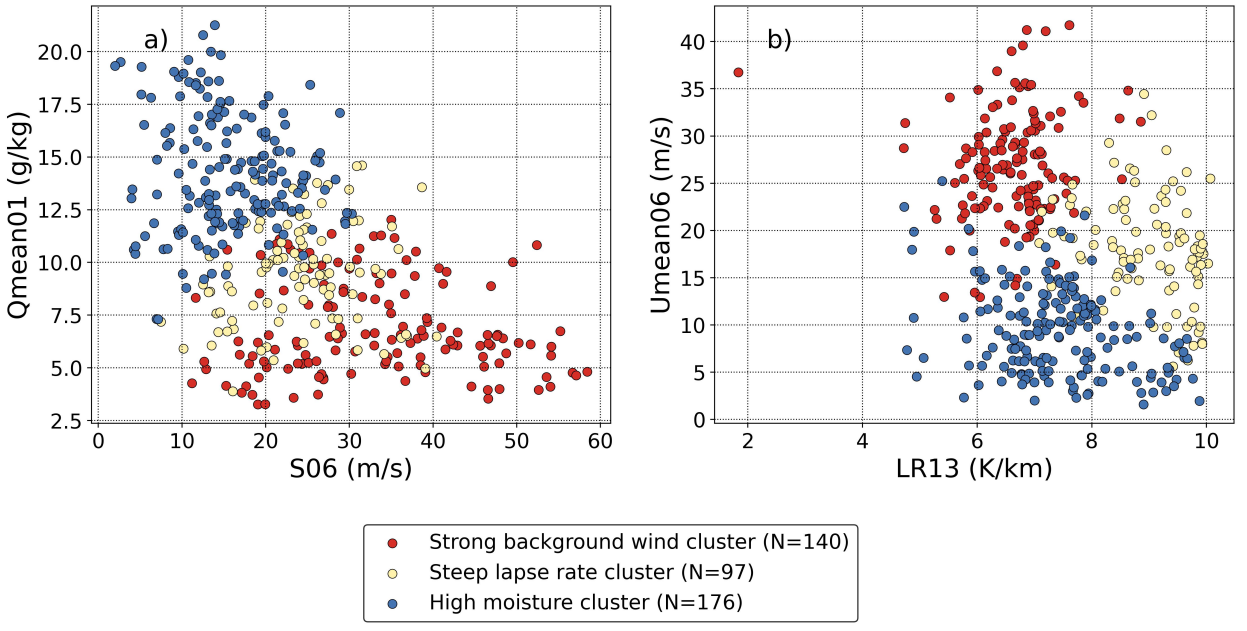

FIG. 2. Scatterplots showing environmental conditions for each severe convective wind event, in terms of a) water vapor mixing ratio from 0–1 km above ground level (Qmean01) and bulk vertical wind shear from 0–6 km above ground level (S06), and b) mean wind speed from 0–6 km above ground level (Umean06) and the temperature lapse rate from 1–3 km above ground level (LR13). Events are colored by type according to environmental clustering (Section 2b), and includes strong background wind (red), steep lapse rate (yellow), and high moisture (blue) event types.

produced by 409 unique parent storms based on radar reflectivity tracking, noting that the tracking algorithm here does not handle splits and mergers such that unique storms could be part of the same broader mesoscale structure. After application of the environmental clustering method described in Section 2b, these 413 events are split into 140 strong background wind, 97 steep lapse rate, and 176 high moisture events. The joint distribution of low-level moisture (Qmean01) and deep-layer wind shear (S06), as well as low-level temperature lapse rate (LR13) and deep-layer mean wind speed (Umean06) reveals that SCW events in Australia exist in a wide range of environmental conditions (Figure 2), consistent with Brown et al. (2023).

Spatial variability is examined here by mapping the proportion of event types that occur in each radar domain (Figure 3). Strong background wind events are observed to occur mostly in southern Australia, with all of these events occurring south of 30-degrees south, and producing the majority of SCW events at coastal locations. This result is expected, given strong synoptic winds are

common in these locations due to high amounts of baroclinicity in the midlatitudes. For locations in tropical Australia, and locations along the east coast, the majority of SCW events are associated with high moisture environments. This is consistent with high moisture availability in the tropics, and the proximity to warm sea surface temperatures for east coast subtropical locations. Although, high moisture events also contribute to a large portion of events in south-eastern Australia. SCW events in steep lapse rate environments tend to occur at inland locations and in south-eastern Australia. Inland locations are where strong surface heating may be expected to provide steep low-level lapse rates, with these environments potentially able to be transported into the south-east in northerly regimes that are commonly observed ahead of synoptic fronts. However, steep lapse rate events are not limited to these locations, and do occur along the east coast and non-coastal tropical locations as shown in Figure 3. Some spatial variability in event types can be observed within radar domains, as demonstrated for Melbourne and Sydney locations in the Supplementary Material (Section S.4). This could be due to siting of individual AWSs, or spatial variability in environments due to proximity to the coastline, for example.

There is significant variability in the total number of events observed between each radar domain, due to availability of wind gust data and the length of the archived radar period (see Table 1). Normalising by the period of available wind gust data in each radar period (events per AWS-years, Table 1), a median value of 0.21 is observed, with lower and upper quartile values accross domains of 0.12 and 0.34, respectively. In other words, SCWs would be expected to occur on average every 5 years at a point location, based on the events here. Some variability in this normalised frequency may also be present: for example, events appear to occur more frequently (normalised by AWS-years) at inland locations (Kalgoorlie, Yarrawonga, Namoi), and less frequently in north-east Australia (Cairns, Townsville, Weipa). A lower number of events in far north-east Australia appears consistent with other studies (Brown and Dowdy 2021a; Spassiani and Mason 2021).

Temporal variability of SCW events is demonstrated within Figure 4, in terms of the relative frequency of SCW occurrence across event types for each month of the year and for each hour of the day, compared with the relative frequency of non-severe events. For example, the red bars in Figure 4a show the frequency of a strong background wind SCW event occurring for a given month, relative to all SCW events at all locations, while the red lines/circles show the same but for non-severe events. There are clear differences in the timing of events from each event type

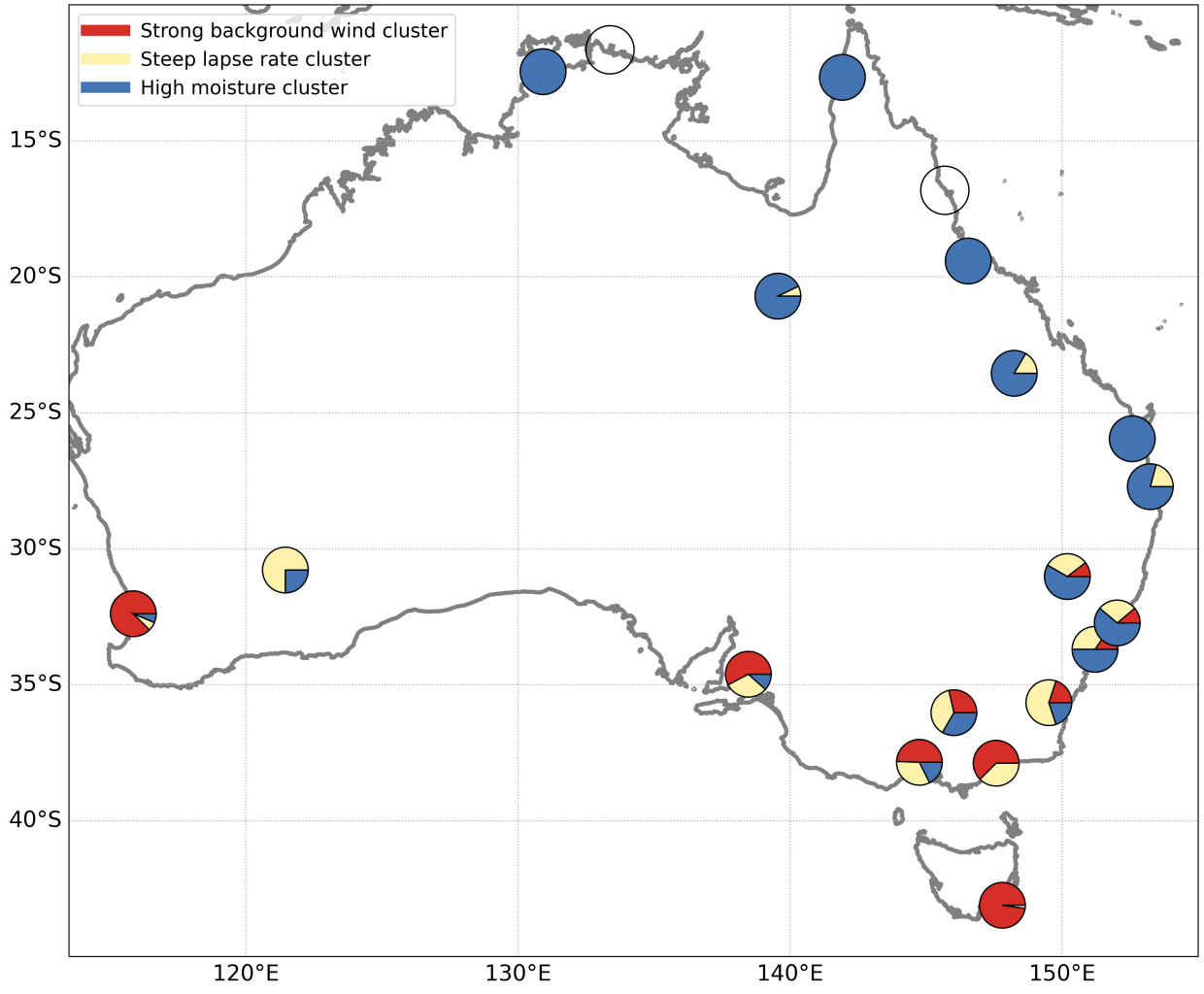

FIG. 3. Proportion of severe convective wind event types at each radar location, including for strong background wind (red), steep lapse rate (yellow) and high moisture (blue) events. Open circles indicate radar locations where no SCW events were observed.

throughout the year, with high moisture and steep lapse rate events peaking in frequency during the warm season, and strong background wind events peaking during the cool season.

The diurnal cycle of SCW occurrences (Figure 4b) suggests that the relative frequency associated with all event types peaks during the mid-afternoon, around the time of maximum daytime surface heating, as expected based on previous studies in Australia (Brown and Dowdy 2021a; Geerts 2001). However, because events within the strong background wind cluster are often driven by synoptic-scale forcing, there is less of an afternoon peak in probability for those events, compared

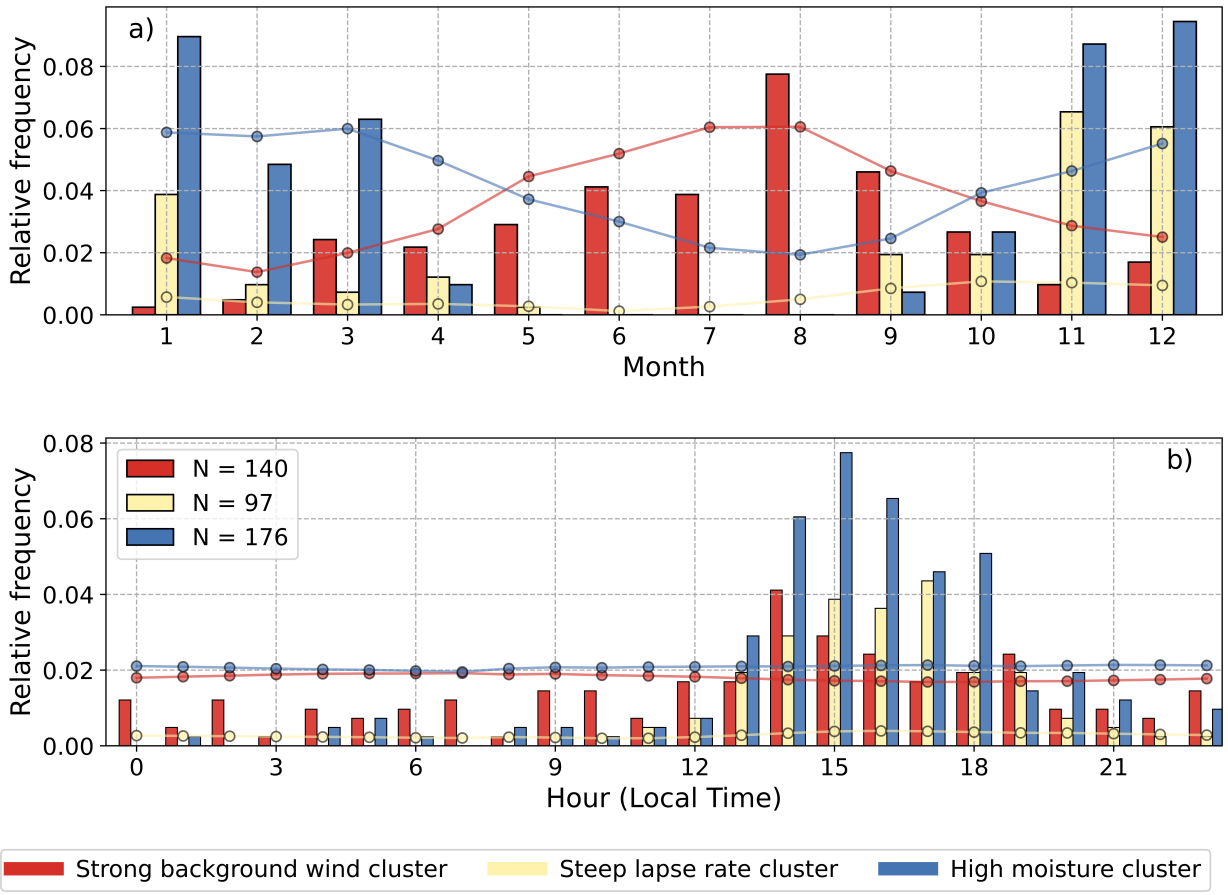

418 FIG. 4. Frequency of severe convective wind (SCW) occurrences for each event type and (a) month of the year
419 (b) hour of the day, relative to all SCW occurrences. Event types are separated based on environmental clustering
420 of SCW events, shown by colors. Relative frequencies for non-severe events are shown by the circle markers and
421 solid lines to aid comparison. The number of SCW events used is shown in a legend in (b), separately for each
422 event type.

428 with the other environmental clusters that are associated with relatively high amounts convective
429 instability (Section 2b). It follows that for south coast locations, there is a less pronounced diurnal
430 cycle in event frequency, compared with locations that have predominately high moisture or steep
431 lapse rate events (seasonal and diurnal variations are shown separately for each location grouping
432 in the Supplementary Material, Section S.5). The frequency of non-severe events for each cluster
433 shows little variation on diurnal time scales, as shown by lines/circles on Figure 4b.

434 Based on the methods used here, 0.003% of all gust events are classed as SCW events, with
435 0.080% of convective gust events classed as SCW events (Table 3). As SCW events and non-

	SCW measurement frequency	
	Relative to all events	Relative to convective events
Event type		
All events	0.003%	0.080%
Strong background wind	0.003%	0.075%
Steep lapse rate	0.012%	0.239%
High moisture	0.003%	0.061%

TABLE 3. The frequency of a severe convective wind (SCW) event being measured (expressed in percentages), calculated relative to all gust events, and relative to convective gust events.

severe events are based on gust observations resampled to hourly intervals (Section 2a), these results represent hourly event frequencies. Event frequencies are lowest for SCWs in the strong background wind and high moisture clusters, and this is the case relative to all events (0.003% for both clusters) and convective events (0.075% and 0.061%, respectively). Frequencies are highest for SCW events in the steep lapse rate cluster (0.012% relative to all events, and 0.239% relative to convective events).

Table 4 shows that the probability of a SCW event being associated with at least one lightning stroke within 50 km and 1 hour is much higher (69.0%) than for convective non-severe events (23.0%) and all non-severe events (2.5%), as expected based on understanding of convective hazards including wind gusts (Reap and MacGorman 1988). However, the probability of lightning occurrence is significantly greater for events that are associated with deep moist convection, in steep lapse rate (80.4%) and high moisture (96.0%) environments, compared with events in strong background wind environments (27.1%) that are often associated with relatively shallow convection (Section 2b, Table 2). This has significant implications for the use of lightning as a proxy for SCW occurrence, such as biasing this method towards identifying steep lapse rate and high moisture events.

b. Wind gust characteristics

Distributions of wind gust statistics for SCW events and convective non-severe events are shown in Figure 5, separately for each event type. These include statistics measured by AWS, such as peak intensity, the peak-to-mean gust ratio, and the ratio of peak wind gust to mid-level wind speed, as well as storm speed estimated from radar data (Section 2d). The speed of the storm is investigated

	Lightning probability		
	SCW events	Convective non-severe events	All non-severe events
Event type			
All events	69.0%	23.0%	2.5%
Strong background wind	27.1%	7.4%	0.5%
Steep lapse rate	80.4%	30.8%	3.4%
High moisture	96.0%	32.0%	4.2%

TABLE 4. The probability of at least one lightning stroke associated with each event type, calculated for severe convective wind (SCW) events, convective non-severe events, and all non-severe events.

here given that it is one component that determines the ground-relative speed of the storm outflow, which can impact the intensity of the resulting surface gust (Sherburn et al. 2021). Storm speed is related to several potential factors, including advection by steering winds, cold-pool or gravity wave propagation, and internal pressure perturbations in some cases, with the contribution of these factors likely varying between event types here (see Supplementary Material Section S.6). Also, by investigating the gust-to-mid-level-wind-speed ratio, the extent to which downwards transport of horizontal mid-level momentum contributes to surface wind speed can be estimated, relative to momentum generated by convective downdraft processes (Section 2d). However, it is noted that the gusts measured by AWS used here may not sample the strongest gust associated with a storm, and peak gust intensity is likely higher in most cases.

The distribution of wind gust intensity for SCW events is largely similar between event types (Figure 5a). However, the steep lapse rate cluster as compared with other clusters has slightly higher median values, a longer upper tail, and includes the three most intense gusts in this dataset (see Supplementary Material Section S.7). This suggests that steep lapse rates may be a key factor for generating the most extreme SCWs in this dataset, resulting in regional variations in extreme gust speeds as demonstrated in the Supplementary Material (Section S.7).

There are significant differences in the distribution of storm speeds between clusters (Figure 5b), likely related to differences in the distribution of Umean06 (see Figure 2). This could be due to the role of steering winds on storm motion, with strong background wind and steep lapse rate events having relatively large median values of storm speed, compared with high moisture events (Figure 5b). The distribution of storm speed is shifted to higher values for SCW events in all clusters compared with convective non-severe events, demonstrating a strong link between

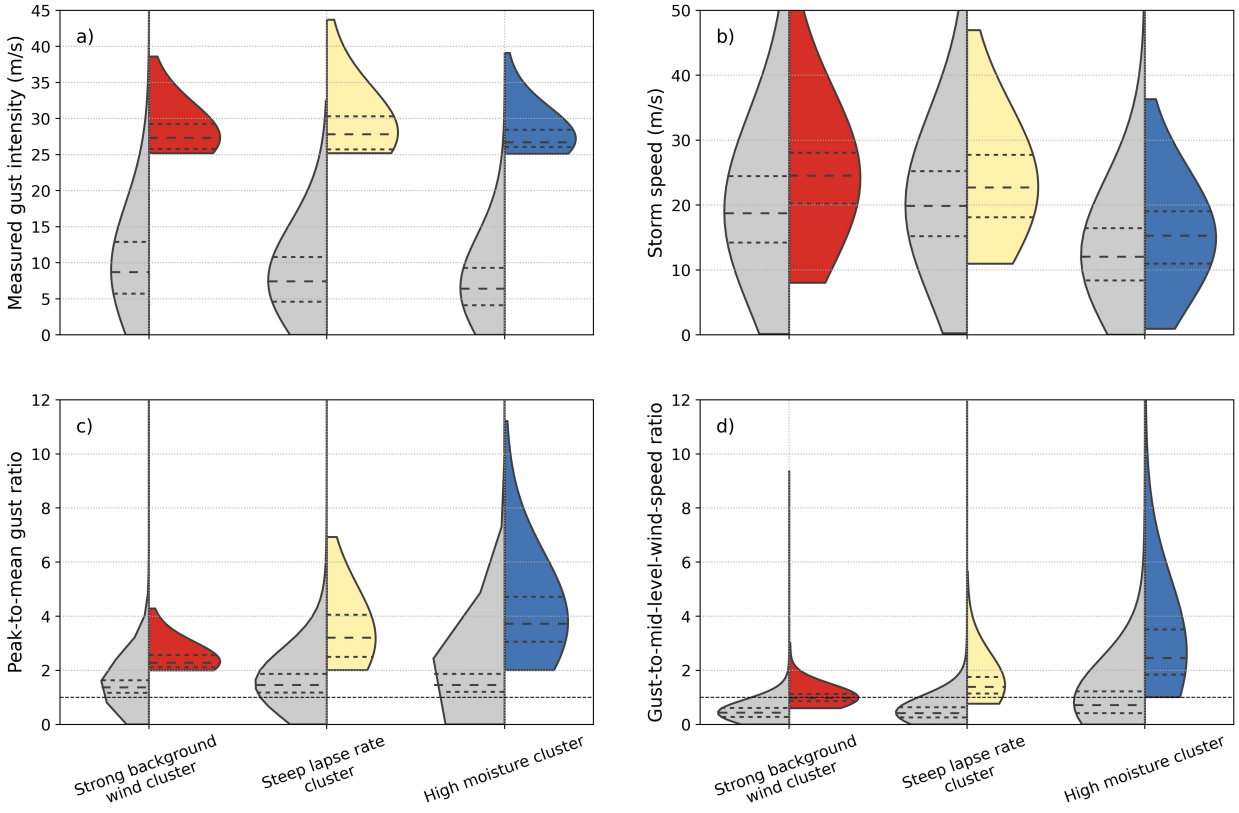

471 FIG. 5. Distribution of wind gust characteristics for each event type, shown for SCW events (coloured
472 distributions) and convective non-severe events (grey distributions). This includes a) the measured gust intensity,
473 b) parent-storm speed, c) the ratio of the gust to the 4-hour mean, and d) the ratio of the gust to the mid-level
474 wind speed. Distributions are estimated by a kernel density estimate approach, and cut-off at the maximum and
475 minimum observed values, to maintain discontinuities such as the threshold for a SCW event at 25 m/s in (a).
476 Within each distribution, inner lines represent quartiles. Horizontal dashed lines in (c) and (d) represent a ratio
477 of 1.

490 background winds, storm speeds, and SCWs, likely due to enhanced downwards momentum
491 transport associated with strong background winds, that also creates fast storm motion.

492 The peak-to-mean gust ratio is significantly higher for SCW events associated with the steep
493 lapse rate and high moisture environments, relative to the strong background wind events. Higher
494 peak-to-mean ratios represent relatively intense, transient gust events. Lower ratios for the strong
495 background wind cluster reflect the presence of strong synoptic systems (low-pressure and frontal
496 systems) during those events, supplying relatively intense wind gusts for the 4-hour mean window.

Similarly, the gust-to-mid-level-wind-speed ratio tends to be higher for events associated with the high moisture cluster, followed by the steep lapse rate and strong background wind clusters (Figure 5d). For the strong background wind cluster, median values for this ratio are around 1.0, with lower and upper quartile values of around 0.9 and 1.1, respectively. This suggests that for 75% of strong background wind events, surface wind gusts are within +/- 10% of the mid-level wind speed, with downwards transport of horizontal momentum from aloft likely being the dominant component of surface wind speed. For the steep lapse rate cluster, median values of the gust-to-mid-level-wind-speed ratio are around 1.4, with lower and upper quartiles of 1.1 and 1.8, respectively. This suggests that for 75% of cases in that cluster, the measured surface wind gust is around 10-80% stronger than the mid-level wind speed. It follows that momentum generated by thermodynamic and dynamic downdraft processes must contribute significantly to outflow speed and severe surface wind production in that cluster. In the high moisture cluster, median values of this ratio are around 2.5, with lower and upper quartiles of 1.8 and 3.5, respectively. For this cluster, momentum generated by convective downdraft processes represent the dominant processes for severe surface wind speed production, noting that background winds are generally much weaker for high moisture events compared with other clusters (Figure 5b). These results are consistent with the study of SCWs in the United States by Sherburn et al. (2021), who showed that the ratio of gust speed to ground-relative storm outflow speed is higher for severe wind gusts in environments with high amounts of convective available potential energy (CAPE, which is also higher for the high moisture cluster, see Table 2), and lower for events with strong background winds.

c. Storm types and environments

Parent storms are most commonly non-linear (24.8%), followed by cell clusters (21.5%), cells (19.7%), and linear storms (16.1%, see Figure 6a). Parent storms for SCWs are less commonly supercellular (10.0%) or embedded supercells (7.9%). Distributions are broadly similar for each event type, although with some notable differences. For the strong background wind cluster (Figure 6c), there is a higher proportion of SCW events associated with linear storms (22.8%) compared with other clusters, and a much lower proportion of events associated with supercells and embedded supercells (0.8% and 3.1%, respectively). For the steep lapse rate cluster (Figure 6e), the probability distribution for SCW events shows a high proportion of cellular storms relative

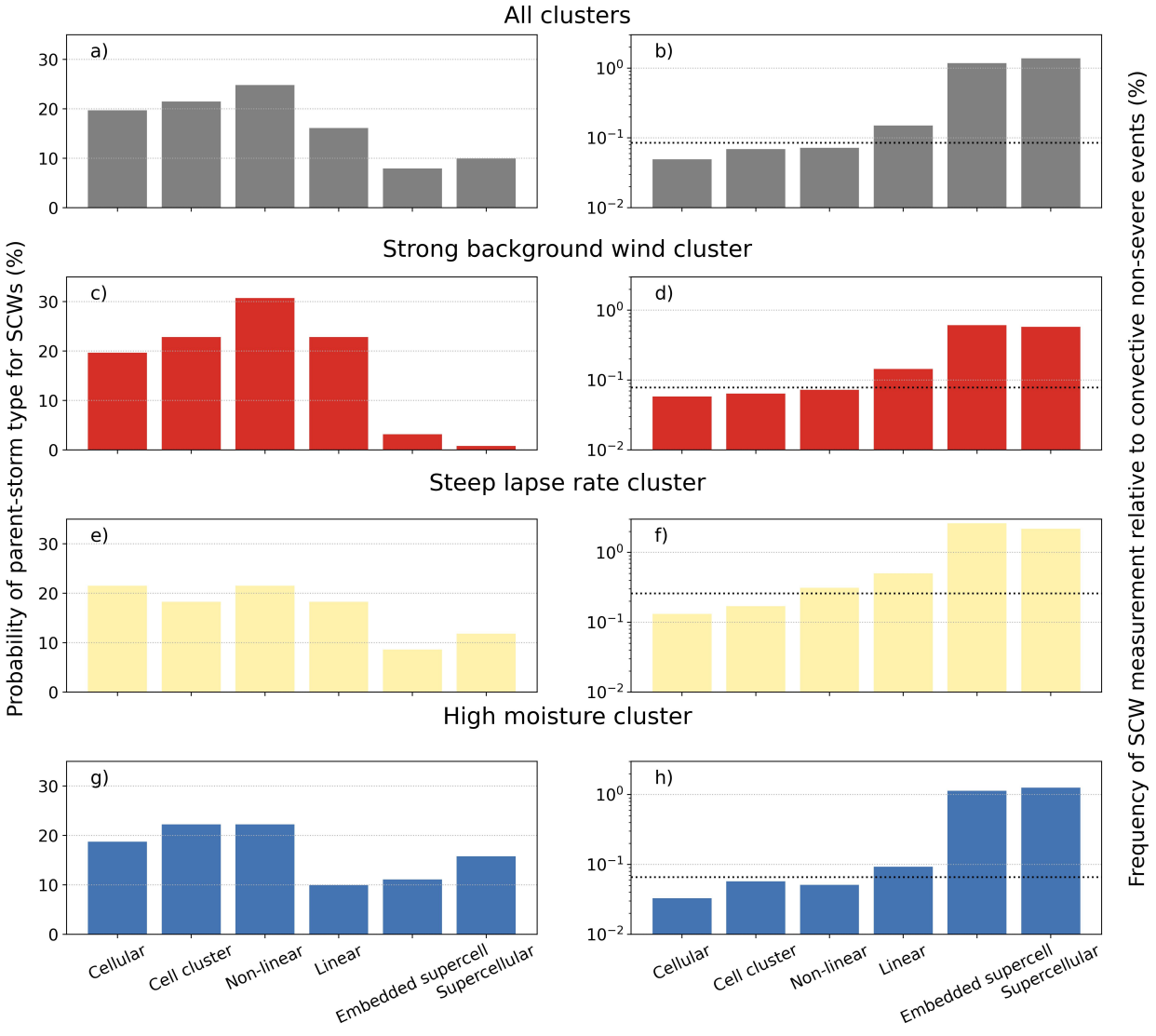

529 FIG. 6. (a,c,e,g) The probability distribution of parent-storm types for SCW events and (b,d,f,h) the frequency
530 of a SCW measurement given the occurrence of each parent-storm type. This is shown for (a,b) all SCW event
531 types combined, as well as (c–h) for each event type individually. Black dotted lines in b, d, f, and h indicate the
532 frequency of SCW measurement given the occurrence of any parent storm, as shown in Table 3. Note that there
533 is a logarithmic scale for in b, d, f, and h.

526 to other parent-storm types. For the high moisture cluster (Figure 6g), there is a lower association
527 of SCW events with linear systems (9.9%) compared with other clusters, and a higher proportion
528 of SCWs that are associated with supercells (15.8%) and embedded supercells (11.1%).

Supercells and embedded supercells have the highest frequency of a SCW event being measured relative to a convective non-severe event (1.40% and 1.19% for supercells and embedded supercells, respectively, see Figure 6b). This is despite having the lowest probability of occurrence amongst SCW events (Figure 6a). The frequency of a SCW event being measured is significantly lower for linear storms (0.15%), followed by non-linear storms and cell-clusters (both 0.07%), and cellular storms (0.05%). Note that the frequency of a SCW event being measured from all storm types is 0.08%, based on the hourly data used here (Table 3). Figure 6d, f, and h indicate little variation in these frequencies between event types, although values are generally higher for steep lapse rate events, compared with other event types, consistent with results shown in Table 3.

Environmental diagnostics are used to investigate differences in the thermodynamic and wind profiles between SCW events and convective non-severe events, for each parent-storm type and for each event type. Consistent with physical understanding, higher values of deep-layer vertical wind shear (S06) are observed for supercellular storms, particularly in the high moisture cluster where the majority of these events occur (Figure 7). However, these distributions for supercell parent storms have some uncertainties, related to the sample size for this storm type, objective classification methods for identifying supercells based on Doppler velocity data, and the choice of deep-layer shear to characterise the vertical wind profile, given that low-level directional shear can also influence supercell development. Notably, around 25% of supercellular events in the high moisture cluster have S06 values less than 15 m/s, with these values not typically expected to support supercell formation. For the steep lapse rate cluster and high moisture cluster, there is very little difference between the SCW S06 distribution and convective non-severe distribution. This suggests that while deep-layer wind shear is associated with storm organisation within these clusters, it might be insufficient for discriminating between SCWs and non-severe events for a given parent-storm type. For the strong background wind cluster, the distribution of S06 for SCW events is shifted to higher values relative to the distribution for convective non-severe events. This could potentially relate to SCW events being associated with relatively strong synoptic systems and large temperature gradients along fronts, for example.

For most parent-storm types in each event type, the distribution of Umean06 is shifted to higher values for SCW events relative to convective non-severe events (Figure 7), as shown already in Section 3b. However, for supercellular and cellular modes in the high moisture cluster, there is

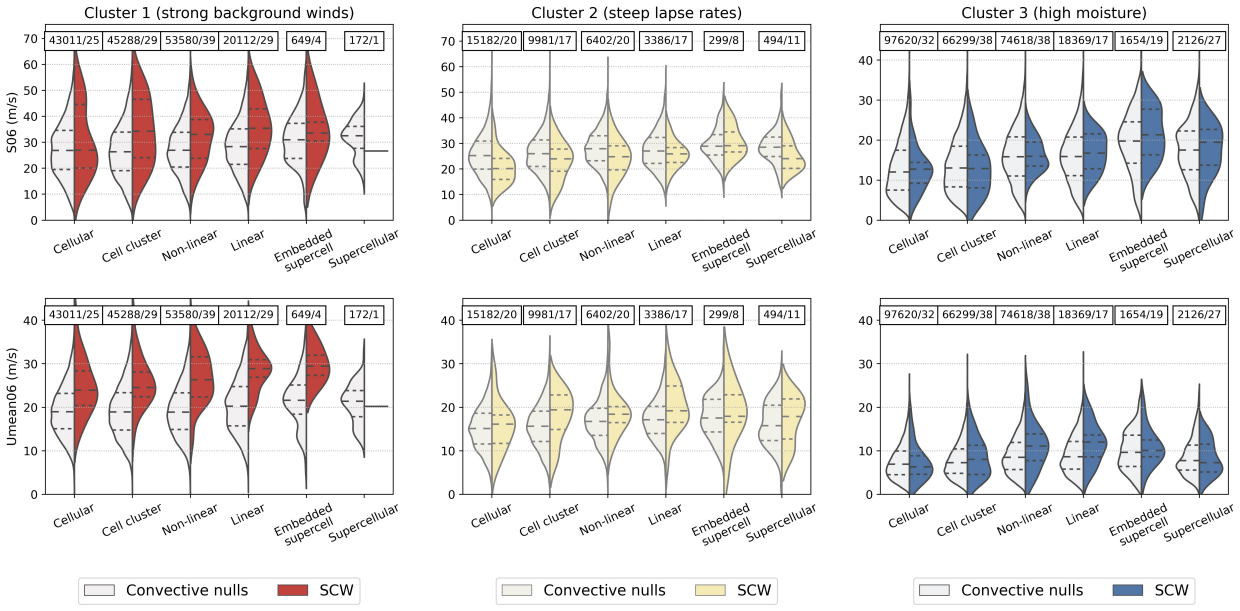

561 FIG. 7. The distribution of wind-related environmental diagnostics for each event type (columns) and parent-
562 storm type, shown separately for SCW events (darker colors) and convective non-severe events (lighter colors).
563 This includes for deep-layer vertical wind shear (S06, top row), and the mean wind speed from 0—6 km
564 (Umean06, bottom row). Distributions are based on a kernel density estimate approach, and the lines within each
565 distribution represent quartiles. The sample size for convective non-severe events (N) and SCW events (M) are
566 shown above each distribution pair, in the form N/M.

570 very little difference between the Umean06 distribution for SCW events and convective non-severe
571 events, suggesting that background winds and momentum transport might not be as relevant for
572 surface wind gusts in these situations. In addition, the difference in Umean06 distributions between
573 SCWs and convective non-severe events is much greater for the strong background wind cluster,
574 compared with the steep lapse rate and high moisture clusters.

575 DCAPE values for SCW events in the high moisture and steep lapse rate clusters are generally
576 much higher compared with the distribution for convective non-severe events, associated with
577 greater potential for downdrafts driven by evaporative cooling, although this shift is more signif-
578 icant for non-supercellular parent-storm types (Figure 8). In contrast, DCAPE distributions are
579 significantly lower for SCW events in the strong background wind cluster, with only a modest
580 increase in median values compared with the distribution for convective non-severe events. Results
581 for MUCAPE are similar to those described for DCAPE: higher values for SCW events compared

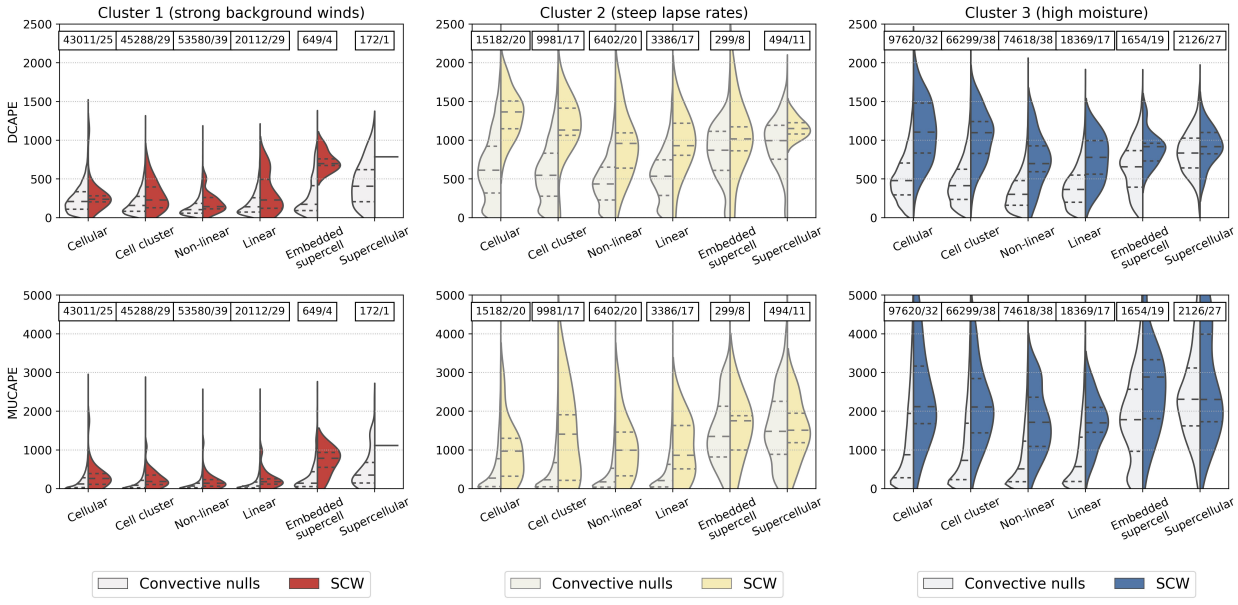

584 FIG. 8. As in Figure 8, but for thermodynamic variables, including downdraft CAPE (DCAPE, top row), and
585 most unstable CAPE (MUCAPE, bottom row).

582 with non-severe events, and most notably in the steep lapse rate and high moisture clusters, and for
583 non-supercellular parent-storm types.

586 These results suggest that in general, environmental wind diagnostics (Umean06 and S06) are
587 potentially more relevant for discriminating between SCW occurrences and non-severe convective
588 gusts in the strong background wind cluster, based on being shifted to higher values for SCW events,
589 while thermodynamic diagnostics (DCAPE and MUCAPE) are potentially useful for discrimination
590 in the steep lapse rate and high moisture clusters. In addition, for supercellular modes, there is
591 potentially reduced discrimination between SCW and convective non-severe events based on the
592 Umean06, CAPE, and DCAPE distributions, compared with other parent-storm types. These
593 results will be investigated further in Section 3d in terms of SCW event discrimination using a
594 wider range of diagnostics based on the AUC score.

595 *d. Environmental diagnostic skill*

596 A set of 48 environmental diagnostics derived from ERA5 data are tested here in their ability
597 to discriminate between SCW events and non-severe events, as well as between SCW events
598 and convective non-severe events. Details for each diagnostic are shown in the Supplementary

Material (Section S.2). Each diagnostic is tested by calculating the AUC score over 1,000 randomly resampled datasets, as described in Section 2e. Firstly, AUC scores are presented for discrimination of SCW and convective non-severe events, and discrimination between SCW events and all non-severe events, for each SCW event type, as well as all events combined (Figure 9). Then, the analysis using convective non-severe events is repeated separately for each parent-storm type (Figure 10). For simplicity, each set of AUC scores is shown for a selection of 10 diagnostics, representing the highest-scoring diagnostics for all events combined. More detailed results for the 10 highest-scoring diagnostics in each event type and parent-storm type are also shown in the Supplementary Material (Section S8).

Considering all event types combined, Figure 9a demonstrates that ConvGust (wet and dry), the Brown and Dowdy (2021a) Statistical Diagnostic (BDSD), and GUSTEX (Geerts 2001) have the highest AUC scores for SCW discrimination compared with convective non-severe events. There is considerable overlap between the AUC distributions for these diagnostics based on random resampling, indicating that differences in AUC scores are not statistically significant to a high degree. Differences in skill between diagnostics appear to become significant after the fifth-ranked diagnostic, the 0–3 km temperature lapse rate, LR03 (compare the AUC distribution between ConvGust (dry) and LR03).

Formulations of the BDSD, GUSTEX, and ConvGust can be found in the Supplementary Material (Section S.2), and are also qualitatively described here. The BDSD combines several environmental variables, including the mean mid-level wind speed, deep-layer wind shear and helicity, the low-level temperature lapse rate, and measures of low-level moisture and instability. The relatively high AUC score for this diagnostic is consistent with results reported by Brown and Dowdy (2021a) based on measured SCW events in Australia, that were defined by wind gusts over 25 m/s with lightning used to infer convective processes. To assess potential overfitting, a cross-validated test of this diagnostic is also presented in Figure 9a (BDSD (CV)). This test only uses data from 2019–2020, completely independent of the 2005–2018 period used to train the diagnostic in Brown and Dowdy (2021a). BDSD (CV) has a similar AUC score to BDSD, suggesting that this statistical diagnostic is not overfit. GUSTEX was developed based on downbursts in eastern Australia by Geerts (2001). It depends on the wind speed at 500 hPa, as well as various measures of moisture content and lapse rates below the melting level. ConvGust (wet and dry) is a diagnostic used

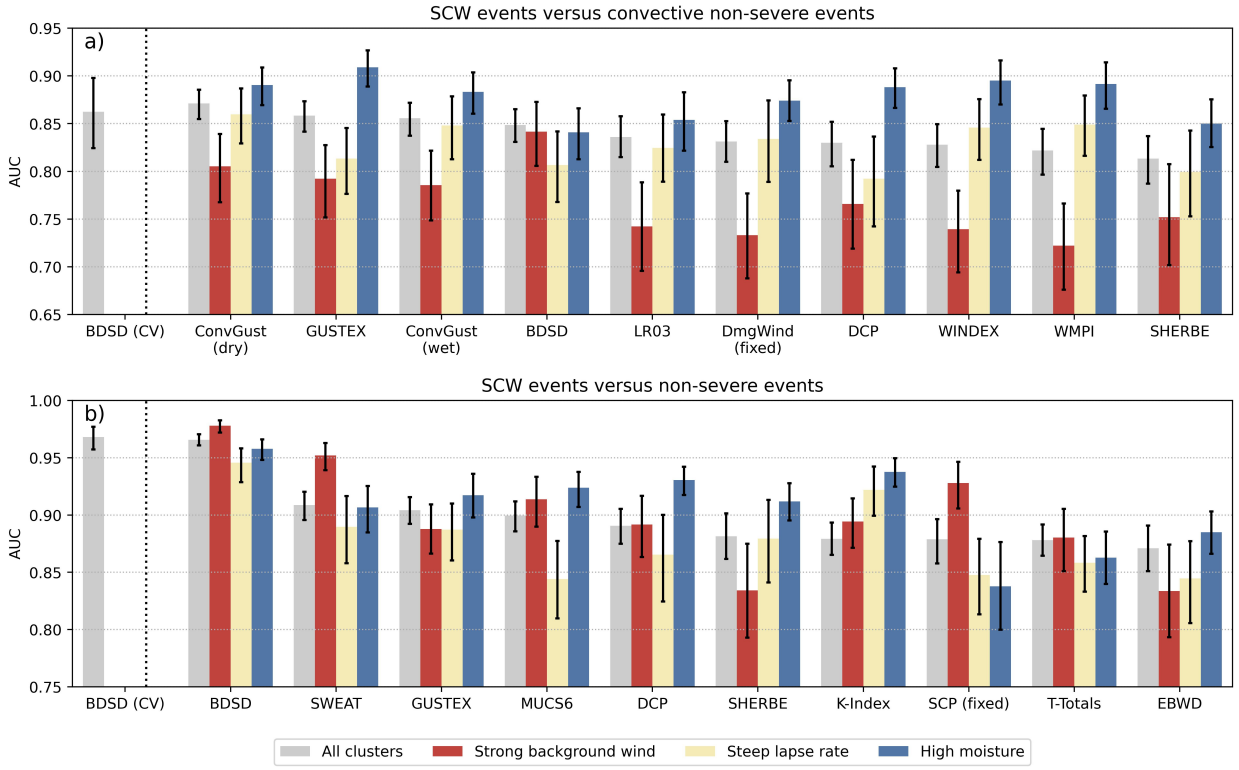

FIG. 9. Area under the ROC curve (AUC) scores for top-performing environmental diagnostics for SCW event discrimination, compared with (a) convective non-severe events and (b) non-severe events. Bars show median AUC scores based on random resampling (Section 2e), with error bars indicating the 95th percentile range over those samples. AUC scores are shown separately for (grey) all event types, (red) strong background wind events, (yellow) steep lapse rate events, and (blue) high moisture events. Diagnostics are sorted by decreasing median AUC scores over all event types. See the main text and Supplementary Material (Section S.2) for diagnostic definitions.

by Australian Bureau of Meteorology severe weather forecasters for downburst prediction, and is intended to estimate the maximum wind gust that could be expected from a wet and dry microburst, respectively. It is defined by the sum of the mean wind speed from 800–600 hPa and DCAPE, with different weightings of DCAPE depending on if a wet or dry microburst is expected.

There are significant differences in the relative discrimination skill of diagnostics accross event types. The BDSD is relatively skillful in discriminating between SCW events and convective non-severe events within the strong background wind cluster compared with other diagnostics (red bars in Figure 9a), while ConvGust (dry and wet) is relatively skilful for the steep lapse rate cluster

(yellow bars in Figure 9a), and GUSTEX is relatively skilful for the high moisture cluster (blue bars in Figure 9a). ROC curves also suggest that optimal thresholds for SCW discrimination may vary to a large degree between event types, as demonstrated in the Supplementary Material for the BDSD (Section S.2).

Considering SCW discrimination compared with all non-severe events (rather than only convective non-severe events), the BDSD is the most skillful diagnostic out of the set considered within all event types (Figure 9b). ConvGust and GUSTEX have much lower relative skill in this case compared with the BDSD (with ConvGust not appearing in the top-10 here for all events combined). This suggests that these diagnostics are most useful when conditioned on storm occurrences, as demonstrated in Figure 9a for example.

For SCW events associated with linear, non-linear, and cell cluster storms, results are similar to those discussed above, namely that the BDSD, ConvGust (wet and dry), and GUSTEX are amongst the most skillful diagnostics for SCW discrimination (Figure 10). However, AUC scores for SCW events associated with cellular storms reveal that the temperature lapse rate from the surface to 3 km above ground level (LR03) provides potentially more skillful discrimination than other diagnostics, and suggests that wind information (such as mean wind speeds included in ConvGust, for example) are less relevant for this storm class. Figure 10 also demonstrates that the skill for supercellular SCW discrimination is much lower than for other parent-storm types. This could be related to relevant physical processes that aren't diagnosed here from the large-scale environment, such as internal pressure perturbations, as well as potentially narrow spatial footprints for supercell rear-flank downdrafts. For both the supercell and embedded supercell class, LR03 again provides relatively good discrimination compared with other diagnostics. However, there are large uncertainties in relative AUC scores based on the number of samples here, as evidenced by the overlap in distributions between diagnostics. Other diagnostics might also be relevant for SCW discrimination associated with supercellular storms, with low-level humidity variables scoring relatively well (see Supplementary Material, Section S.8).

4. Discussion

Severe convective winds (SCWs) are investigated here within 20 radar domains around Australia, with a clustering technique applied to identify different types of events based on the large-scale

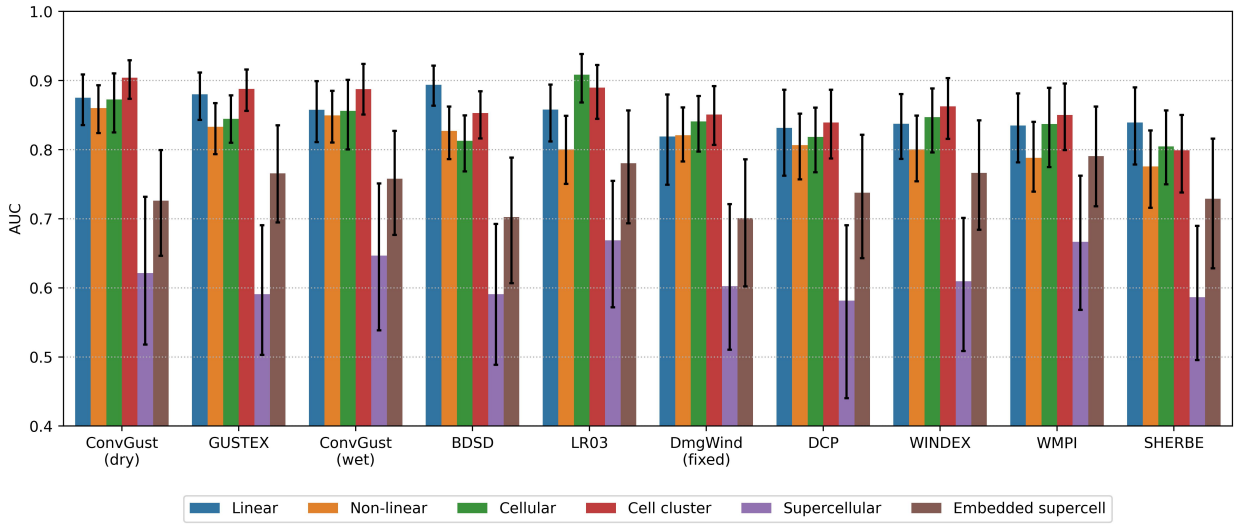

FIG. 10. As in Figure 9, but split between different parent-storm types, rather than different SCW event types.

convective environment. These different event types are associated with strong background wind, steep lapse rate, and high moisture environments (Section 2b). In addition, we also further classify SCW events in each cluster according to the type of parent storm, based on radar data. These clustering and classification methods allow for the investigation of how SCW characteristics vary with different event types, with results related to these characteristics discussed here as follows.

SCWs are measured here with a relative frequency of 0.004% compared with all gust events, and 0.080% compared with convective gust events, based on hourly data, with a median value across station locations of 0.21 events per year of AWS measurements. Events associated with steep lapse rate environments have a much higher probability of being measured compared with other event types (see Table 3). Seasonally, these types of events are shown to peak in occurrence during the late spring/early summer, and generally occur in southeast and inland locations. Similarly, high moisture events tend to peak in the summer, and most often occur at locations along the east coast, and in the tropics.

Peak event occurrence in the warm season for steep lapse rate and high moisture events is consistent with other studies in Australia that focus on SCWs in general, as well as other convective hazards associated with deep moist convection (Allen and Karoly 2014; Brown and Dowdy 2021a). The earlier seasonal peak in steep lapse rate events compared with high moisture events confirms the findings of Geerts (2001), who showed that the seasonal distribution of short-lived SCWs

(lasting less than 10-minutes), which were assumed in that study to be associated with air-mass thunderstorms with high surface temperatures, is shifted towards late spring, compared with longer-lived SCWs that were shown in that study to peak in summer, and assumed to be associated with organised severe thunderstorms. This was reasoned by Geerts (2001) to relate to the earlier peak in surface temperatures throughout the year, supportive of steep low-level lapse rates, compared to the annual peak in moisture availability. The current study has extended these findings through the use of classification methods to define SCW event types.

In contrast to events in the steep lapse rate and high moisture clusters, strong background wind events are shown to occur mostly in the cool season, and in southern coastal locations, likely due to enhanced baroclinicity in these locations. This seasonal variation is consistent with previous studies that have investigated convective hazards in environments with low amounts of instability in the United States (Sherburn and Parker 2014), and cool-season tornadoes in Australia (Kounkou et al. 2009). These previous studies have shown that cool-season convective hazards often occur with high amounts of vertical wind shear, and this is also the case for SCW events in the strong background wind cluster (see Figure 2).

Results here demonstrate for the first time that there is large variability in the fraction of SCW events associated with lightning between event types. Of the events associated with the strong background wind cluster, only 27% have lightning within 50 km and 1 hour, compared with 80% for steep lapse rate events, and 96% for the high moisture events. This is consistent with strong background wind events being associated with relatively shallow convection, and low amounts of convective instability, compared with other clusters (see Table 2). It is therefore likely that approaches for identifying SCWs using lightning are biased towards events that are associated with relatively deep convective processes.

There are some notable differences in wind gust statistics between event types, suggesting potentially different physical processes responsible for severe surface winds, consistent with their definition based on different environmental conditions. For example, following similar analysis by Sherburn et al. (2021), low gust-to-mid-level-wind-speed ratios for the strong background wind cluster suggests that the convective transport of horizontal momentum to the surface is a significant component of severe surface wind production. In contrast, high gust-to-mid-level-wind-speed ratios for the high moisture and steep lapse rate clusters suggests that thermodynamic processes,

such as strong downdrafts due to the evaporation and melting of precipitation, are a more important mechanism for severe wind production. These findings support Geerts (2001) who suggest that convective transport of horizontal momentum from aloft is important to consider for downburst prediction, although the importance of this might vary with environmental conditions as shown in the results here.

The steep lapse rate cluster has a wind gust intensity distribution with an upper tail shifted to higher values relative to other clusters, with three relatively extreme gusts over 40 m/s. While studies have shown that convective wind gust intensities have different statistical properties to non-convective gusts (Holmes 2002), the results here suggest that there may also be different statistical properties for different convective wind types. This idea has also been suggested by Lombardo et al. (2014), based on a variety of temporal gust characteristics from a set of thunderstorm cases. However, it should be noted that there are significant uncertainties in differences between wind gust intensity distributions, especially for the upper tail, based on a relatively small sample size here and measurements from point locations that will underestimate the maximum gust produced from a storm in most cases.

SCW events are shown here to occur in association with different parent-storm types based on radar data, with notable variations in the frequency of storm types between environmental clusters. Smith et al. (2013) found that disorganised (that is, neither linear or supercellular) storms were associated with 47% of measured SCWs in the United States, while linear modes were associated with 42%, and supercells 11%. These results can be compared with the results here, with 66% of events associated with disorganised storms (including cells, cell clusters, and non-linear types), with a lower number of events associated with linear storms (16%) and a similar amount of supercellular storms to Smith et al. (2013) (18% including both supercells and embedded supercells). The proportion of linear storms associated with SCW events here is relatively low compared to Smith et al. (2013), in addition to other studies such as Gatzen (2013) and Klimowski et al. (2003), who find that linear storms are the dominant mode of SCW production in Germany, and the high plains of the United States, respectively. The low proportion of linear storms here could be related to the size of the radar domains used here for storm identification (with a radial radar range of around 150 km), compared with the length threshold for a linear system (100 km). Differences between the results here and previous studies may also relate to different classification schemes and methods for storm

identification, with manual analysis used in previous studies compared with the objective methods here. Linear systems are observed here to occur more frequently in association with SCWs in the strong background wind and steep lapse rate environmental clusters, with these clusters having lower CAPE and higher Umean06 compared with the high moisture cluster (Table 2). This is consistent with Pacey et al. (2021) who show that for SCWs in the United Kingdom, linear systems are more often observed in cool-season, low-CAPE environments, compared with warm-season high-CAPE environments. Physically, the higher frequency of linear SCW events in the cool-season may relate to shallow convective lines or frontal rain bands, associated with synoptic-scale frontal boundaries (Clark 2013). In contrast, supercellular modes are more often associated with SCWs in the high moisture cluster that generally occur during the summer, consistent with Smith et al. (2013) who found that the association between SCWs and supercells peaks in summer in the United States.

For discriminating between SCWs and convective non-severe events within strong background wind environments, the statistical diagnostic of Brown and Dowdy (2021a) (BDSD) is shown to be relatively skillful compared with other commonly used diagnostics for downburst prediction. In addition, thermodynamic variables provide relatively little discrimination for these events in strong background wind environments (Figure 8) as compared with wind variables (Figure 7). For steep lapse rate and high moisture events, diagnostics intended for downburst and microburst prediction are relatively skillful, such as GUSTEX (Geerts 2001) and ConvGust (see Supplementary Material Section S.2 for definitions). The results for these latter event types are similar to other studies that have investigated the usefulness of various convective diagnostics for SCW discrimination. This includes Dotzek and Friedrich (2009), who found that GUSTEX can identify downburst environments in Germany, and Kuchera and Parker (2006), who found that the DmgWind diagnostic investigated here, which has a similar formulation to the ConvGust diagnostic mentioned above (see Supplementary Material Section S.2), has skillful discrimination for widespread convective windstorms in the United States. Consistent with differences in wind gust statistics discussed earlier, these results suggest that different physical processes are responsible for severe wind production between event types, with variations in skill between SCW diagnostics potentially reflecting these different processes. Furthermore, the BDSD is shown to be most useful when discriminating between SCW events and all non-severe events, rather than non-severe events conditioned on storm

occurrence. This finding may be relevant in situations where storm information is absent, such as identification of SCW environments from large-scale climate model data.

The highest amount of discrimination between cellular SCW events and convective non-severe events is based on using low-level lapse rates (from 0–3 km) as a diagnostic. This could potentially reflect different physical mechanisms associated with SCWs from cellular storms, compared with other parent-storm types. The usefulness of low-level lapse rates for cellular storms is consistent with many previous modelling and observational studies for downburst events (Proctor 1989; Wakimoto 1985; Romanic et al. 2022). It is noted that the environmental diagnostics used in this study for SCW identification are based on global ERA5 data, used to identify large-scale conditions associated with SCW events. Future work could investigate the role of convection-allowing models for SCW identification, including performance for different event types, with these models able to partially resolve convective processes.

There are several limitations to this study that should be kept in mind when interpreting the results and discussions presented here. Firstly, there are uncertainties related to sampling surface winds associated with a storm, with underestimations likely here using AWS measurements at point locations. In addition, this might be exaggerated for certain types of events with small spatial footprints, such as supercell downdrafts or microbursts. Secondly, there is potential for parent-storm type misclassifications using the objective approach outlined in Section 2c. Limitations related to this parent-storm type classification method have been discussed by Brown et al. (2023), and are related in particular to storm segmentation using a reflectivity threshold, and supercellular classifications based on azimuthal shear. Next, there are uncertainties related to how global reanalysis products, such as ERA5 used here for event clustering and calculating diagnostics, can represent the convective environment. ERA5 has been shown to have significant biases compared with rawinsonde observations, particularly for parcel-based diagnostics and composite indices (Taszarek et al. 2020b), but is judged to be suitable for use here based on its use by previous studies for studying convective diagnostics (Taszarek et al. 2020b; Romanic et al. 2022; Zhou et al. 2021), as well as providing value by having global spatial coverage at hourly resolution. Finally, we have used differences in environments, diagnostic skill, and wind gust distributions between event types to infer different physical processes related to measured severe surface winds, without direct observation of these processes. This includes suggesting a greater role for convective transport

of horizontal momentum within the strong background wind clusters, compared with the high moisture cluster, based on the gust-to-mid-level-wind-speed ratio, for example. Future work could build on the results here, by using a combination of high-resolution modelling and observations to characterise different physical processes between event types.

5. Conclusion

Long-term characteristics of three different severe convective wind (SCW) event types were analysed. The study dataset comprised 413 SCW events at 20 weather radar locations around Australia, based on automatic weather station, radar, lightning, and reanalysis data . Event types were defined by statistical clustering of environmental conditions, including SCWs associated with strong background winds, steep lapse rates, and high low-level moisture, as defined by a previous study in this region (Brown et al. 2023). Key findings are listed as follows for each of the four key research questions posed in the Introduction:

- *How frequently do different types of SCWs occur in Australia and does this vary spatially and seasonally?*

  SCW events are measured most frequently for steep lapse rate environments, followed by strong background wind and high moisture environments. Strong background wind events tend to occur in southern Australia, with a peak occurrence frequency around the late Austral winter. Steep lapse rate events tend to occur in south-east Australia and at inland locations, with a peak occurrence frequency during the late Austral spring. High moisture events tend to occur along the east coast of Australia and in tropical regions, with a peak occurrence frequency during the Austral summer.

- *How do the SCW types differ in their wind gust characteristics and parent storm types?*

  The ratio of gust speed to mean wind speed is generally higher for high moisture and steep lapse rate events, compared with strong background wind events. This implies that there may be differences in the relative contribution of thermodynamic and dynamic storm processes and downwards momentum transport for SCW production between event types. The most extreme wind gust intensities (+ 40 m/s) occurred for the steep lapse rate cluster. It was also found that supercellular parent storms are least commonly associated with SCW events, compared

with cellular, linear, and non-linear storms, but have highest relative frequency of a measured SCW when they do occur.

- *What is the probability of lightning occurrence associated with each type of SCW event?*

  There is significant variability in the probability of lightning occurrence associated with each type of SCW event. A relatively low proportion of strong background wind events (27%) are associated with at least one lightning stroke within 1-hour and 50 km, compared with steep lapse rate (80%) and high moisture (96%) events.

- *What are the relevant diagnostics for discriminating between SCWs and non-severe events, and do these vary between types of SCW events and types of parent storms?*

  Diagnostics from reanalysis data that are based on environmental wind speeds appear to be relatively skillful for discriminating between SCW events and convective non-severe events within the strong background wind cluster, compared with thermodynamic diagnostics for SCWs. Diagnostics intended for downburst prediction, that combine wind speeds aloft with estimates of convective downdraft intensity, are most skillful for discriminating between SCWs and convective non-severe events within the steep lapse rate and high moisture clusters. This includes GUSTEX (Geerts 2001), and ConvGust (product of downdraft convective available potential energy and mid-level wind speeds). When considering discrimination between SCWs and all non-severe events (not just convective non-severe events), the statistical diagnostic of Brown and Dowdy (2021a) is most skillful for all event types. The skill of different environmental diagnostics for SCW discrimination also varies with parent-storm type, most notably for events associated with cellular storms and supercells.

The results presented in this study are intended to provide insights on SCW events in Australia, with several potential applications. Assessments of diagnostic skill are intended to be useful for weather forecasting applications in this region based on environmental approaches that identify the relevant ingredients for SCWs, where the diagnostics that are relevant may depend on the type of event as demonstrated here. Similarly, the results here have demonstrated that multiple diagnostic approaches may be required to study climatological conditions leading to SCWs, given the diversity in SCW types. Further, these results also demonstrate that predictions of extreme wind speeds for engineering design may depend on different types of storms and convective processes, given that

some types of environments tend to produce more extreme wind speeds than others. In addition, this study has shown that the probability of lightning occurrence varies with SCW event type, and this is significant because SCWs are often defined by lightning occurrences in climatological studies (Yang et al. 2017; Mohr et al. 2017; Brown and Dowdy 2021a), and lightning is also sometimes used in nowcasting applications for SCWs (Thompson et al. 2021). Finally, this study has documented the spatial and temporal variability in SCW event types around Australia, as well as the distribution of parent-storm types and wind gust statistics, with these results intended to improve understanding of the physical processes that lead to different SCW events, building on studies of SCWs in other regions around the world.

Acknowledgments. AB and TL are supported by the Australian Research Council's (ARC) Centre of Excellence for Climate Extremes (CE170100023). SH is supported by the ARC Discovery Program (project DP200102516). AD is supported by the National Environmental Science Program. Comments on earlier versions of this manuscript by Rob Taggart and Callum Stuart are gratefully acknowledged, as well as comments from three anonymous reviewers. Processing and tracking of radar data was made possible by various python software, including tobac (Heikenfeld et al. 2019), TINT (Raut et al. 2021), and scipy (Virtanen et al. 2020). Processing of environmental diagnostics was made possible by various python software, including MetPy (May et al. 2019), wrf-python (Ladwig 2017), and SkewT (https://pypi.org/project/SkewT/). We acknowledge computational support and resources from the National Computational Infrastructure.

Data availability statement. Hourly maximum wind gust data, as well as associated parent-storm information, and environmental diagnostics, are available for the locations used in this study in a Zenodo archive managed by the authors: https://zenodo.org/record/7474859. Information on access to WWLLN lightning data can be found from http://wwlln.net, while information on access to station wind gust observations collected by the Australian Bureau of Meteorology can be found at http://www.bom.gov.au/climate/data/stations/. The ERA5 reanalysis data used here is openly available from the Australian National Computing Infrastructure (NCI, http://dx.doi.org/10.25914/5fb115b82e2ba). The Australian Unified Radar Archive is also openly available on NCI (https://dx.doi.org/10.25914/5f4c85732ee80).

References

Allen, J. T., and E. R. Allen, 2016: A review of severe thunderstorms in Australia. *Atmospheric Research*, **178-179**, 347–366, https://doi.org/10.1016/j.atmosres.2016.03.011, URL http://dx.doi.org/10.1016/j.atmosres.2016.03.011.

Allen, J. T., and D. J. Karoly, 2014: A climatology of Australian severe thunderstorm environments 1979 – 2011 : Inter-annual variability and ENSO influence. *International Journal of Climatology*, **34**, 81–97, https://doi.org/10.1002/joc.3667.

Atkins, N. T., and R. M. Wakimoto, 1991: Wet Microburst Activity over the Southeastern United States: Implications for Forecasting. *Weather and Forecasting*, **6 (4)**, 470–482, https://doi.org/10.1175/1520-0434(1991)006⟨0470:WMAOTS⟩2.0.CO;2, URL http://journals.ametsoc.org/doi/10.1175/1520-0434(1991)006%3C0470:WMAOTS%3E2.0.CO;2.

Australian Energy Market Operator, 2020: Preliminary Report – Victoria and South Australia Separation Event, 31 January 2020. Tech. rep.

Bolgiani, P., D. Santos-Muñoz, S. Fernández-González, M. Sastre, F. Valero, and M. L. Martín, 2020: Microburst Detection With the WRF Model: Effective Resolution and Forecasting Indices. *Journal of Geophysical Research: Atmospheres*, **125 (14)**, https://doi.org/10.1029/2020JD032883.

Brown, A., and A. Dowdy, 2021a: Severe convection-related winds in Australia and their associated environments. *Journal of Southern Hemisphere Earth System Science*, https://doi.org/10.1071/ES19052, URL https://doi.org/10.1071/ES19052.

Brown, A., and A. Dowdy, 2021b: Severe Convective Wind Environments and Future Projected Changes in Australia. *Journal of Geophysical Research: Atmospheres*, **126 (16)**, 1–17, https://doi.org/10.1029/2021JD034633, URL https://onlinelibrary.wiley.com/doi/10.1029/2021JD034633.

Brown, A., A. Dowdy, T. P. Lane, and S. Hitchcock, 2023: Types of Severe Convective Wind Events in Eastern Australia. *Monthly Weather Review*, **151 (2)**, 419–448, https://doi.org/10.1175/MWR-D-22-0096.1, URL https://journals.ametsoc.org/view/journals/mwre/aop/

MWR-D-22-0096.1/MWR-D-22-0096.1.xmlhttps://journals.ametsoc.org/view/journals/mwre/151/2/MWR-D-22-0096.1.xml.

Cintineo, J. L., M. J. Pavolonis, J. M. Sieglaff, L. Cronce, and J. Brunner, 2020: Noaa probsevere v2.0—probhail, probwind, and probtor. *Weather and Forecasting*, **35 (4)**, 1523–1543, https://doi.org/10.1175/WAF-D-19-0242.1.

Clark, M. R., 2013: A provisional climatology of cool-season convective lines in the UK. *Atmospheric Research*, **123**, 180–196, https://doi.org/10.1016/j.atmosres.2012.09.018, URL http://dx.doi.org/10.1016/j.atmosres.2012.09.018.

De Gaetano, P., M. P. Repetto, T. Repetto, and G. Solari, 2014: Separation and classification of extreme wind events from anemometric records. *Journal of Wind Engineering and Industrial Aerodynamics*, **126**, 132–143, https://doi.org/10.1016/j.jweia.2014.01.006, URL http://dx.doi.org/10.1016/j.jweia.2014.01.006.

Dotzek, N., and K. Friedrich, 2009: Downburst-producing thunderstorms in southern Germany: Radar analysis and predictability. *Atmospheric Research*, **93 (1-3)**, 457–473, https://doi.org/10.1016/j.atmosres.2008.09.034, URL http://dx.doi.org/10.1016/j.atmosres.2008.09.034.

Dowdy, A., and A. Brown, 2023: Environmental indicators for thunderstorms , lightning and convective rainfall. Tech. Rep. Bureau Research Report No. 077, Australian Bureau of Meteorology. URL http://www.bom.gov.au/research/publications/researchreports/BRR-077.pdf.

Durañona, V., M. Sterling, and C. J. Baker, 2007: An analysis of extreme non-synoptic winds. *Journal of Wind Engineering and Industrial Aerodynamics*, **95 (9-11)**, 1007–1027, https://doi.org/10.1016/j.jweia.2007.01.014.

Earl, N., S. Dorling, M. Starks, and R. Finch, 2017: Subsynoptic-scale features associated with extreme surface gusts in UK extratropical cyclone events. *Geophysical Research Letters*, **44 (8)**, 3932–3940, https://doi.org/10.1002/2017GL073124, URL https://onlinelibrary.wiley.com/doi/10.1002/2017GL073124.

Earl, N., and I. Simmonds, 2018: Sub synoptic-scale features associated with extreme surface gusts during the South Australia Storm of September 2016 - Part II: analysis of mechanisms driving the gusts. *Weather*, https://doi.org/10.1002/wea.3384, URL http://doi.wiley.com/10.1002/wea.3384.

El Rafei, M., S. Sherwood, J. P. Evans, and F. Ji, 2023: Analysis of extreme wind gusts using a high-resolution Australian Regional Reanalysis. *Weather and Climate Extremes*, **39 (December 2022)**, 100 537, https://doi.org/10.1016/j.wace.2022.100537, URL https://doi.org/10.1016/j.wace.2022.100537.

Fujita, T. T., 1983: "Andrews AFB Microburst," by Fujita, T. Theodore, SMRP Research Paper 205. Tech. rep. URL https://swco-ir.tdl.org/handle/10605/262003.

Gallus, W. A., N. A. Snook, and E. V. Johnson, 2008: Spring and Summer Severe Weather Reports over the Midwest as a Function of Convective Mode: A Preliminary Study. *Weather and Forecasting*, **23 (1)**, 101–113, https://doi.org/10.1175/2007WAF2006120.1, URL https://journals.ametsoc.org/doi/10.1175/2007WAF2006120.1.

Gatzen, C. P., 2013: Warm-season severe wind events in Germany. *Atmospheric Research*, **123**, 197–205, https://doi.org/10.1016/j.atmosres.2012.07.017, URL http://dx.doi.org/10.1016/j.atmosres.2012.07.017.

Geerts, B., 2001: Estimating Downburst-Related Maximum Surface Wind Speeds by Means of Proximity Soundings in New South Wales, Australia. *Weather and Forecasting*, **16 (2)**, 261–269, https://doi.org/10.1175/1520-0434(2001)016⟨0261:EDRMSW⟩2.0.CO;2, URL http://journals.ametsoc.org/doi/abs/10.1175/1520-0434%282001%29016%3C0261%3AEDRMSW%3E2.0.CO%3B2.

Gilmore, M. S., and L. J. Wicker, 1998: The Influence of Midtropospheric Dryness on Supercell Morphology and Evolution. *Monthly Weather Review*, **126 (4)**, 943–958, https://doi.org/10.1175/1520-0493(1998)126⟨0943:TIOMDO⟩2.0.CO;2, URL http://journals.ametsoc.org/doi/10.1175/1520-0493(1998)126%3C0943:TIOMDO%3E2.0.CO;2.

Goodman, S. J., D. E. Buechler, P. D. Wright, and W. D. Rust, 1988: Lightning and precipitation history of a microburst-producing storm. *Geophysical Research Letters*, **15 (11)**, 1185–1188, https://doi.org/10.1029/GL015i011p01185, URL http://doi.wiley.com/10.1029/GL015i011p01185.

Heikenfeld, M., P. J. Marinescu, M. Christensen, D. Watson-Parris, F. Senf, S. C. van den Heever, and P. Stier, 2019: tobac 1.2: towards a flexible framework for tracking and analysis of clouds

in diverse datasets. *Geoscientific Model Development*, **12 (11)**, 4551–4570, https://doi.org/10.5194/gmd-12-4551-2019, URL https://gmd.copernicus.org/articles/12/4551/2019/.

Hersbach, H., and Coauthors, 2020: The ERA5 Global Reanalysis. *Quarterly Journal of the Royal Meteorological Society*, qj.3803, https://doi.org/10.1002/qj.3803, URL https://onlinelibrary.wiley.com/doi/abs/10.1002/qj.3803.

Hitchcock, S. M., T. P. Lane, R. A. Warren, and J. S. Soderholm, 2021: Linear rainfall features and their association with rainfall extremes near Melbourne, Australia. *Monthly Weather Review*, https://doi.org/10.1175/mwr-d-21-0007.1.

Hogan, R. J., and I. B. Mason, 2011: Deterministic forecasts of binary events. *Forecast Verification : A Practitioner's Guide in Atmospheric Science*, I. T. Jolliffe, and D. B. Stephenson, Eds., second edi ed., John Wiley & Sons, Ltd.

Holmes, J., 2002: A Re-analysis of Recorded Extreme Wind Speeds in Region A. *Australian Journal of Structural Engineering*, **4 (1)**, 29–40, https://doi.org/10.1080/13287982.2002.11464905, URL https://www.tandfonline.com/action/journalInformation?journalCode=tsen20https://www.tandfonline.com/doi/full/10.1080/13287982.2002.11464905.

Jesson, M., M. Sterling, C. Letchford, and C. Baker, 2015: Aerodynamic forces on the roofs of low-, mid- and high-rise buildings subject to transient winds. *Journal of Wind Engineering and Industrial Aerodynamics*, **143**, 42–49, https://doi.org/10.1016/j.jweia.2015.04.020, URL http://dx.doi.org/10.1016/j.jweia.2015.04.020.

Johns, R. H., and W. D. Hirt, 1987: Derechos: Widespread Convectively Induced Windstorms. *Weather and Forecasting*, **2 (1)**, 32–49, https://doi.org/10.1175/1520-0434(1987)002⟨0032:dwciw⟩2.0.co;2.

Keenan, T. D., and R. E. Carbone, 1992: A Preliminary Morphology of Precipitation Systems In Tropical Northern Australia. *Quarterly Journal of the Royal Meteorological Society*, **118 (504)**, 283–326, https://doi.org/10.1002/qj.49711850406.

Klemp, J. B., and R. Rotunno, 1983: A Study of the Tornadic Region within a Supercell Thunderstorm. *Journal of the Atmospheric Sciences*, **40 (2)**, 359–377, https://doi.org/https://doi.org/10.1175/1520-0469(1983)040⟨0359:ASOTTR⟩2.0.CO;2.

Klimowski, B. A., M. J. Bunkers, M. R. Hjelmfelt, and J. N. Covert, 2003: Severe convective windstorms over the northern High Plains of the United States. *Weather and Forecasting*, **18 (3)**, 502–519, https://doi.org/10.1175/1520-0434(2003)18⟨502:SCWOTN⟩2.0.CO;2.

Kounkou, R., G. Mills, and B. Timbal, 2009: A reanalysis climatology of cool-season tornado environments over southern Australia. *International Journal of Climatology*, **29 (14)**, 2079–2090, https://doi.org/10.1002/joc.1856, URL http://doi.wiley.com/10.1002/joc.1856.

Kuchera, E. L., and M. D. Parker, 2006: Severe Convective Wind Environments. *Weather and Forecasting*, **21 (4)**, 595–612, https://doi.org/10.1175/waf931.1.

Ladwig, W., 2017: wrf-python (Version 1.1.0) [Software]. UCAR/NCAR, Boulder, Colorado, URL https://doi.org/10.5065/D6W094P1.

Lagerquist, R., A. McGovern, and T. Smith, 2017: Machine Learning for Real-Time Prediction of Damaging Straight-Line Convective Wind. *Weather and Forecasting*, **32 (6)**, 2175–2193, https://doi.org/10.1175/WAF-D-17-0038.1, URL https://journals.ametsoc.org/doi/10.1175/WAF-D-17-0038.1.

Lombardo, F. T., D. A. Smith, J. L. Schroeder, and K. C. Mehta, 2014: Thunderstorm characteristics of importance to wind engineering. *Journal of Wind Engineering and Industrial Aerodynamics*, **125**, 121–132, https://doi.org/10.1016/j.jweia.2013.12.004, URL http://dx.doi.org/10.1016/j.jweia.2013.12.004.

Lombardo, F. T., and A. S. Zickar, 2020: Prediction of Non-Synoptic Wind Speeds. *The Oxford Handbook of Non-Synoptic Wind Storms*, September.

Mahoney, K. M., G. M. Lackmann, and M. D. Parker, 2009: The role of momentum transport in the motion of a quasi-idealized mesoscale convective scale. *Monthly Weather Review*, **137 (10)**, 3316–3338, https://doi.org/10.1175/2009MWR2895.1.

May, R. M., S. C. Arms, P. Marsh, E. Bruning, J. R. Leeman, K. Goebbert, J. E. Thielen, and Z. Bruck, 2019: MetPy: A Python Package for Meteorological Data. Unidata, Boulder, Colorado, URL https://github.com/Unidata/MetPy, https://doi.org/10.5065/D6WW7G29.

Miller, P. W., and T. L. Mote, 2018: Characterizing severe weather potential in synoptically weakly forced thunderstorm environments. *Natural Hazards and Earth System Sciences*, **18 (4)**, 1261–1277, https://doi.org/10.5194/nhess-18-1261-2018.

Mohr, S., M. Kunz, A. Richter, and B. Ruck, 2017: Statistical characteristics of convective wind gusts in Germany. *Natural Hazards and Earth System Sciences*, **17 (6)**, 957–969, https://doi.org/10.5194/nhess-17-957-2017, URL https://nhess.copernicus.org/articles/17/957/2017/.

Morgenstern, D., I. Stucke, G. J. Mayr, A. Zeileis, and T. Simon, 2023: Thunderstorm environments in Europe. *Weather and Climate Dynamics*, **4 (2)**, 489–509, https://doi.org/10.5194/wcd-4-489-2023, URL https://wcd.copernicus.org/articles/4/489/2023/.

Pacey, G. P., D. M. Schultz, and L. Garcia-Carreras, 2021: Severe Convective Windstorms in Europe: Climatology, Preconvective Environments, and Convective Mode. *Weather and Forecasting*, **36 (1)**, 237–252, https://doi.org/10.1175/WAF-D-20-0075.1, URL https://journals.ametsoc.org/view/journals/wefo/36/1/WAF-D-20-0075.1.xml.

Peter, J. R., M. J. Manton, R. Potts, P. T. May, S. M. Collis, and L. Wilson, 2015: Radar-derived statistics of convective storms in southeast Queensland. *Journal of Applied Meteorology and Climatology*, **54 (10)**, 1985–2008, https://doi.org/10.1175/JAMC-D-13-0347.1.

Potts, R. J., B. Hanstrum, and P. Dunda, 2010: Sydney Airport Wind Shear Encounter - 15 April 2007. *AMS 14th Conference on Aviation, Range, and Aerospace Meteorology*, Atlanta, GA, URL https://ams.confex.com/ams/90annual/techprogram/paper_163510.htm.

Proctor, F. H., 1989: Numerical simulations of an isolated microburst. Part II: sensitivity experiments. *Journal of the Atmospheric Sciences*, **46 (14)**, 2143–2165, https://doi.org/10.1175/1520-0469(1989)046⟨2143:NSOAIM⟩2.0.CO;2.

Rasmussen, E. N., and D. O. Blanchard, 1998: A baseline climatology of sounding-derived supercell and tornado forecast parameters. *Weather and Forecasting*, **13 (4)**, 1148–1164, https://doi.org/10.1175/1520-0434(1998)013⟨1148:ABCOSD⟩2.0.CO;2.

Raut, B. A., R. Jackson, M. Picel, S. M. Collis, M. Bergemann, and C. Jakob, 2021: An adaptive tracking algorithm for convection in simulated and remote sensing data. *Journal of Applied Meteorology and Climatology*, **60 (4)**, 513–526, https://doi.org/10.1175/JAMC-D-20-0119.1.

Reap, R. M., and D. R. MacGorman, 1988: Cloud-to-ground lightning: Climatological characteristics and relationships to model fields, radar observations, and severe local storms. *Monthly Weather Review*, **117**, 518–535.

Richter, H., J. Peter, and S. Collis, 2014: Analysis of a Destructive Wind Storm on 16 November 2008 in Brisbane, Australia. *Monthly Weather Review*, **142 (9)**, 3038–3060, https://doi.org/10.1175/mwr-d-13-00405.1.

Richter, H., J. Soderholm, J. Taylor, and A. Protat, 2016: Doppler radar and storm environment observations of a maritime tornadic supercell in Sydney, Australia. *28th AMS Conference on Severe Local Storms, Portland, Oregon, American Meteorological Society*.

Romanic, D., M. Taszarek, and H. Brooks, 2022: Convective environments leading to microburst , macroburst and downburst events across the United States. *Weather and Climate Extremes*, **37 (June)**, 100 474, https://doi.org/10.1016/j.wace.2022.100474, URL https://doi.org/10.1016/j.wace.2022.100474.

Savory, E., G. A. Parke, M. Zeinoddini, N. Toy, and P. Disney, 2001: Modelling of tornado and microburst-induced wind loading and failure of a lattice transmission tower. *Engineering Structures*, **23 (4)**, 365–375, https://doi.org/10.1016/S0141-0296(00)00045-6.

Sherburn, K. D., M. J. Bunkers, and A. J. Mose, 2021: Radar-Based Comparison of Thunderstorm Outflow Boundary Speeds versus Peak Wind Gusts from Automated Stations. *Weather and Forecasting*, 1–50, https://doi.org/10.1175/waf-d-20-0221.1.

Sherburn, K. D., and M. D. Parker, 2014: Climatology and Ingredients of Significant Severe Convection in High-Shear, Low-CAPE Environments. *Weather and Forecasting*, **29 (4)**, 854–877, https://doi.org/10.1175/WAF-D-13-00041.1, URL https://journals.ametsoc.org/doi/10.1175/WAF-D-13-00041.1.

Sherman, D. J., 1987: The Passage of a Weak Thunderstorn Downburst over an Instrumented Tower. *Monthly Weather Review*, **115 (6)**, 1193–1205, URL https://doi.org/10.1175/1520-0493(1987)115%3C1193:TPOAWT%3E2.0.CO;2.

Short, E., T. P. Lane, and C. L. Vincent, 2022: Objectively Diagnosing Characteristics of Mesoscale Organization from Radar Reflectivity and Ambient Winds. *Monthly Weather Review*, **151 (3)**, 643–662, https://doi.org/10.1175/mwr-d-22-0146.1.

Smith, B. T., T. E. Castellanos, A. C. Winters, C. M. Mead, A. R. Dean, and R. L. Thompson, 2013: Measured Severe Convective Wind Climatology and Associated Convective Modes of Thunderstorms in the Contiguous United States, 2003–09. *Weather and Forecasting*, **28 (1)**, 229–236, https://doi.org/10.1175/WAF-D-12-00096.1, URL https://journals.ametsoc.org/doi/10.1175/WAF-D-12-00096.1.

Soderholm, J., V. Louf, J. Brook, and A. Protat, 2022: Australian Operational Weather Radar Level 1b Dataset. National Computing Infrastructure, https://doi.org/10.25914/40KE-NM05.

Soderholm, J. S., H. McGowan, H. Richter, K. Walsh, T. M. Weckwerth, and M. Coleman, 2017: An 18-year climatology of hailstorm trends and related drivers across southeast Queensland, Australia. *Quarterly Journal of the Royal Meteorological Society*, **143 (703)**, 1123–1135, https://doi.org/10.1002/qj.2995.

Spassiani, A. C., and M. S. Mason, 2021: Application of Self-organizing Maps to classify the meteorological origin of wind gusts in Australia. *Journal of Wind Engineering and Industrial Aerodynamics*, **210 (January)**, 104 529, https://doi.org/10.1016/j.jweia.2021.104529, URL https://doi.org/10.1016/j.jweia.2021.104529.

Su, C.-H., N. Eizenberg, D. Jakob, P. Fox-Hughes, P. Steinle, C. White, and C. Franklin, 2020: BARRA v1.0: Kilometre-scale downscaling of an Australian regional atmospheric reanalysis over four midlatitude domains. *Geoscientific Model Development Discussions*, **(December)**, 1–34, https://doi.org/10.5194/gmd-2020-366.

Taszarek, M., J. T. Allen, T. Púčik, K. A. Hoogewind, and H. E. Brooks, 2020a: Severe convective storms across Europe and the United States. Part 2: ERA5 environments associated with lightning, large hail, severe wind and tornadoes. *Journal of Climate*, 1–53, https://doi.org/10.1175/JCLI-D-20-0346.1, URL https://journals.ametsoc.org/jcli/article/354770/Severe-convective-storms-across-Europe-and-the.

Taszarek, M., N. Pilguj, J. T. Allen, V. Gensini, H. E. Brooks, and P. Szuster, 2020b: Comparison of convective parameters derived from ERA5 and MERRA2 with rawinsonde data over Europe and North America. *Journal of Climate*, 1–55, https://doi.org/10.1175/JCLI-D-20-0484.1, URL https://journals.ametsoc.org/view/journals/clim/aop/JCLI-D-20-0484.1/JCLI-D-20-0484.1.xml.

Thompson, K. B., M. G. Bateman, and J. R. Mecikalski, 2021: Signatures of Oceanic Wind Events in Geostationary Cloud Top Temperature and Lightning Data. *Weather and Forecasting*, **36 (2)**, 407–423, https://doi.org/10.1175/WAF-D-19-0214.1, URL https://journals.ametsoc.org/view/journals/wefo/36/2/WAF-D-19-0214.1.xml.

Tory, K. J., and W. Thurston, 2015: Pyrocumulonimbus: a Literature Review. Tech. rep., Bushfire and natural hazards CRC, Australia.

van den Broeke, M. S., D. M. Schultz, R. H. Johns, J. S. Evans, and J. E. Hales, 2005: Cloud-to-ground lightning production in strongly forced, low-instability, convective lines associated with damaging wind. *Weather and Forecasting*, **20 (4)**, 517–530, https://doi.org/10.1175/WAF876.1.

Virtanen, P., and Coauthors, 2020: SciPy 1.0: Fundamental Algorithms for Scientific Computing in Python. *Nature Methods*, **17**, 261–272, https://doi.org/10.1038/s41592-019-0686-2.

Virts, K. S., J. M. Wallace, M. L. Hutchins, and R. H. Holzworth, 2013: Highlights of a new ground-based, hourly global lightning climatology. *Bulletin of the American Meteorological Society*, **94 (9)**, 1381–1391, https://doi.org/10.1175/BAMS-D-12-00082.1.

Wakimoto, R. M., 1985: Forecasting dry microburst activity over the High Plains. *Monthly Weather Review*, **113**, 1131–1143.

Weisman, M. L., 1992: The Role of Convectively Generated Rear-Inflow Jets in the Evolution of Long-Lived Mesoconvective Systems. *Journal of the Atmospheric Sciences*, **49 (19)**, 1826–1847, https://doi.org/10.1175/1520-0469(1992)049⟨1826:TROCGR⟩2.0.CO;2, URL http://journals.ametsoc.org/doi/10.1175/1520-0469(1992)049%3C1826:TROCGR%3E2.0.CO;2.

Wilks, D. S., 2001: A skill score based on economic value for probability forecasts. *Meteorological Applications*, **8 (2)**, S1350482701002 092, https://doi.org/10.1017/S1350482701002092, URL http://doi.wiley.com/10.1017/S1350482701002092.

Yang, X., and J. Sun, 2018: Organizational Modes of Severe Wind-producing Convective Systems over North China. *Advances in Atmospheric Sciences*, **35 (5)**, 540–549, https://doi.org/10.1007/s00376-017-7114-2.

Yang, X., J. Sun, and Y. Zheng, 2017: A 5-yr Climatology of Severe Convective Wind Events over China. *Weather and Forecasting*, **32 (4)**, 1289–1299, https://doi.org/10.1175/waf-d-16-0101.1.

Zhou, Z., Q. Zhang, J. T. Allen, X. Ni, and C. Ng, 2021: How Many Types of Severe Hailstorm Environments Are There Globally? *Geophysical Research Letters*, **48 (23)**, 1–11, https://doi.org/10.1029/2021GL095485, URL https://onlinelibrary.wiley.com/doi/10.1029/2021GL095485.